

Molecular Reactions of Protein Phosphatases—Insights from Structure and Chemistry

Michael D. Jackson and John M. Denu^{*,†}

Department of Biochemistry and Molecular Biology, Oregon Health Sciences University, 3181 SW Sam Jackson Park Road, Portland, Oregon 97201

Received October 16, 2000

Contents

I. Introduction	2313
II. Protein Tyrosine Phosphatases	2314
A. Structure of the PTP Family	2314
1. Protein Tyrosine Phosphatases	2314
2. Low Molecular Weight Phosphatases	2315
3. Cdc25	2316
B. Important Sequences Outside the Catalytic Domain and Substrate Specificity of PTPs	2316
C. Catalytic Mechanism of Protein Tyrosine Phosphatases	2319
1. Role of the Conserved Cysteine, Arginine, and Aspartate Residues	2319
2. Transition-State Structure and the Role of the Conserved Serine/Threonine Residue in Catalysis	2320
D. Regulatory Mechanisms of Protein Tyrosine Phosphatases	2323
1. Regulation via Intra- or Intermolecular Interactions	2324
2. Oxidative Regulation of the Active-Site Cysteine	2327
3. Regulation by Phosphorylation	2328
III. Serine/Threonine Specific Protein Phosphatases	2329
A. Background	2329
B. The PPP Gene Family	2330
1. Structure of the PPP Gene Family	2330
2. Catalytic Mechanism of the PPP Family	2331
C. The PPM Gene Family	2333
1. Structure of the PPM Family	2333
2. Catalytic Mechanism of the PPM Gene Family	2334
D. Regulation of Serine/Threonine Phosphatases	2336
IV. Mechanistic Comparisons between Protein Phosphatases and Alkaline Phosphatases	2336
V. Acknowledgments	2337
VI. References	2337

I. Introduction

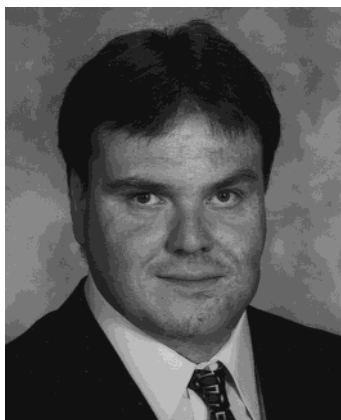
The use of phosphate esters within the cell has a range of applications. These include the use as a source of energy such as in the form of adenosyl

triphosphate (ATP), a means of covalently linking organic molecules synthesized in primary and secondary metabolism, or a mechanism of regulation of protein function via covalent modification of amino acid side chains. The reversible phosphorylation of proteins can result in the activation or termination of many important cellular events including cell signaling, growth, and differentiation.¹ The two classes of proteins that are involved in this reversible process are the protein kinases and protein phosphatases. The protein phosphatases can be divided into two main subclasses based upon their substrate specificity and protein structure.^{2–4} Protein phosphatases (PPs) specifically hydrolyze serine/threonine phosphoesters, while protein tyrosine phosphatases (PTPs) hydrolyze phosphotyrosine. The PTPs can be further classified into phosphotyrosine-specific PTPs and PTPs, which can hydrolyze both phosphotyrosine and serine/threonine phosphoesters (referred to as dual-specificity protein tyrosine phosphatases, DS-PTPs). Each family of phosphatases (the PPs and PTPs) utilizes dramatically different mechanisms to facilitate catalysis. PTPs contain a cysteine nucleophile, which forms an initial enzyme–phosphate intermediate. This intermediate is then hydrolyzed to form inorganic phosphate and the regenerated enzyme. Although less is known about catalysis, PPs contain a dinuclear metal ion center that has been proposed to activate a water molecule for direct hydrolysis of the serine/threonine phosphoester bond.

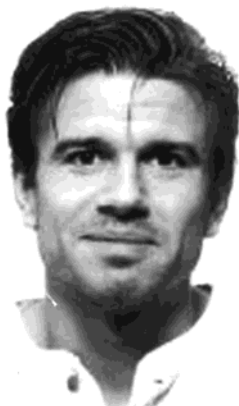
The importance of understanding the protein phosphatases is exemplified by the fact that approximately 150 protein phosphatases are believed to be encoded in the human genome.⁵ Because of their importance and ubiquitous occurrence in nature, biochemical and structural studies have recently explored the mechanism of phosphatase catalysis and regulation. More work in this area is required, however, before a complete mechanistic and regulatory picture of these enzymes is available. Several excellent reviews on the PPs and PTPs have been published within the last several years.^{2,6–12} Many, however, are in the form of minireviews or do not address the entire protein phosphatase family. A review by Barford et al.¹³ does encompass both classes of phosphatases, but new developments, especially in the area of phosphatase structure, mechanism, and regulation, have been published since the release of this review. These recent results provide greater insight into these important classes

* To whom correspondence should be addressed. Phone: (503) 494-0644. Fax: (503) 494-8393. E-mail: denuj@ohsu.edu.

† J.M.D. was supported by NIH Grant GM 59785-01 and American Heart Association Grant 99603442.



Michael D. Jackson was born in Ogden, UT, in 1968. He attended Western Oregon University, where he received his Bachelors degree in Chemistry in 1993. Continuing at Oregon State University, he studied the biosynthesis of secondary natural products with Professor Mark Zabriskie and obtained his Ph.D. degree in Chemistry. His graduate work entailed the study of arginine secondary metabolism in the antibiotic-producing soil bacteria, *Streptomyces lavendulae*. In 2000 he began a postdoctoral fellowship at the Oregon Health Sciences University, working with Dr. John M. Denu on elucidating the catalytic mechanism of the human protein phosphatase, PP2C α . Michael's other academic interests include the study of histone acetylation/deacetylation as well as the development and synthesis of potential inhibitors or substrate analogues to histone deacetylases. Dr. Jackson lives in Salem, OR, with his wife with whom he enjoys biking, hiking, and fishing.



John Denu was born in Beloit, WI, in 1965. He received his Bachelors of Science degree (Biochemistry) in 1988 from the University of Wisconsin—Madison. In 1993 he received his Ph.D. degree in Biochemistry and Biophysics at Texas A&M University under Paul Fitzpatrick. His Ph.D. thesis work focused on understanding the enzymatic mechanism of flavin-containing oxidases. He was a National Institutes of Health postdoctoral fellow under Jack E. Dixon at the University of Michigan—Ann Arbor (Department of Biological Chemistry). At Michigan, Denu studied the structure and function of protein phosphatases. In 1996 he moved to Oregon Health Science University, where he is currently an Assistant Professor of Biochemistry and Molecular Biology. His research interests include understanding the enzymology of signal transduction and gene activation. Currently, his laboratory is focused on understanding the molecular mechanisms of enzymes involved in reversible protein phosphorylation and reversible protein acetylation.

of phosphatases. In this review, the general features of protein phosphatase structure and catalysis for both the PPs and PTPs will be discussed in detail, with greater emphasis on research published since 1997. Also presented is a review of the literature on regulation of PTPs and specific members of the PP class of phosphatases.

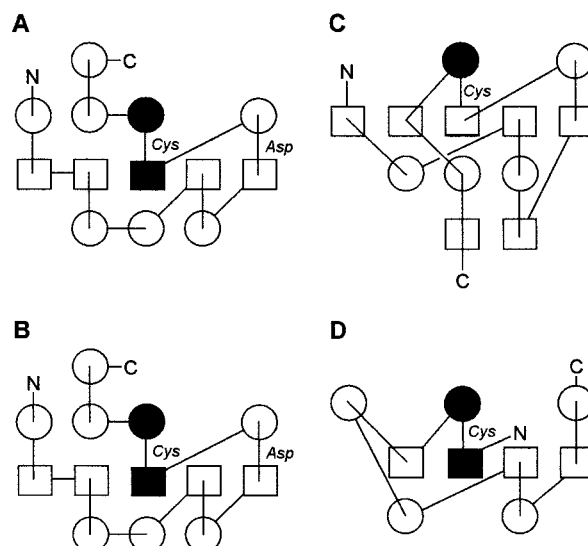


Figure 1. Topological comparisons of three families of PTPs: (A) The dual-specificity PTP VHR, (B) PTEN, (C) Cdc25A, and (D) bovine low molecular weight phosphatase. α -Helixes are represented as circles and β -strands as squares. N and C specify the protein termini. The general location of the cysteine nucleophile (Cys) and general-acid residue (Asp) are presented for both VHR and PTEN.

II. Protein Tyrosine Phosphatases

A. Structure of the PTP Family

1. Protein Tyrosine Phosphatases

There are three topologically distinct protein tyrosine phosphatase families (Figure 1) that share a common active-site motif containing the sequence C(X)₅R(S/T) (single letter amino acid code and X can denote any amino acid). One exception of this general rule is Cdc25, which lacks the serine/threonine residue. The first and largest family includes such members as PTP-1B and *Yersinia* PTP as well as the DS-PTPs VHR (for Vaccinia H1 Related) and the mitogen-activated protein kinase phosphatases (MKPs). The *Yersinia* PTP (Yop51) is a known virulence factor in bacterium responsible for the bubonic plague¹⁴ and is the most active phosphatase known to date.¹⁵ The high catalytic efficiency of the *Yersinia* PTP has made it an excellent model for the study of the catalytic mechanism for the tyrosine-specific protein phosphatases. PTP-1B was originally isolated from human placenta, and while it exhibits only ~20–30% amino acid similarity with the catalytic domain of *Yersinia* PTP,¹⁶ it shows a high degree of structural similarity and has been used as a representative member of the mammalian PTPs. VHR is one of the smallest DS-PTPs, containing only the catalytic domain that is common to all DS-PTPs. This has made VHR an excellent model for studying the catalytic mechanism of DS-PTPs and PTPs. DS-PTPs are further characterized by an extended active-site signature sequence (VXVHCXXGXXRS-(X)₅AY(L/I)M).^{17,18} A second family includes the low molecular weight PTPs (LMW-PTPs), while the third family includes the Cdc25 phosphatases. The catalytic domain of PTPs consists of roughly 250 amino acids. While the PTPs contain as little as 10%

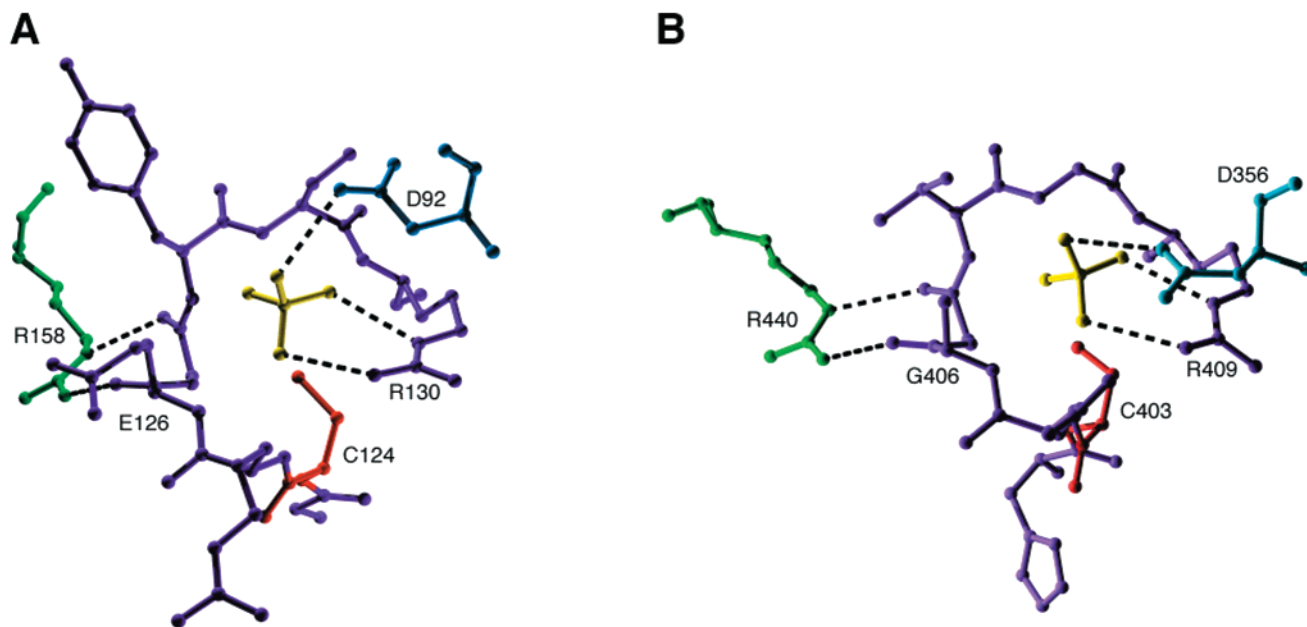


Figure 2. Three-dimensional structure of the signature motifs of (A) VHR and (B) *Yersinia* PTP, illustrating the conserved architecture of the active site utilized by PTPs. The peptide backbone comprising the phosphate-binding loop is purple. The cysteine residues (red) are positioned below the phosphate (yellow, tungstate in *Yersinia* PTP) for S_N2 attack, while a conserved aspartate (blue) is ideally positioned to protonate the leaving group upon departure from the active site. Partial structures were obtained from the crystal structures of VHR and *Yersinia* PTP published by Yuvaniyana et al.¹⁸ and Stuckey et al.,²¹ respectively. Structures were generated using Swiss Pdb Viewer v3.5²³ and POV-Ray v3.1.

identity, the conserved sequences are mostly located within the active site.

Through the solution of several X-ray crystal structures of PTPs and DS-PTPs, a conserved secondary structural scaffold consisting of a single ($\alpha + \beta$)-type domain has been identified (Figure 1).^{18–22} This domain consists of four parallel β strands that are sandwiched by α helices. The phosphate-binding loop (also referred to as the PTP signature motif), which contains the residues C(X)₅R(S/T) (Figures 1 and 2),²³ resides between the β strand starting with C and the α helix beginning with R(S/T). This catalytic region contains a conserved cysteine and arginine residue which are critical for enzyme activity.^{24–27} A highly conserved aspartate residue is also required for catalysis^{28–30} and is located on a separate loop (referred to as the general-acid loop) near the top of the active site. The aspartate residue resides approximately 30–40 residues away from the active-site motif in the primary sequence.

One striking difference between the PTPs and the DS-PTPs resides in the depth of the active-site pocket. In the dual-specificity phosphatase VHR, the depth of the active site is ~ 6 Å deep in comparison to PTP-1B and other PTPs, which have a depth of ~ 9 Å (Figure 2).¹⁸ This difference in the depth of the active site has been proposed to govern, in part, the specificity of PTPs toward phosphotyrosine residues, because the depth of the pocket roughly corresponds to the length of the phosphorylated side chain.

Recently the crystal structure of the putative tumor suppressor phosphatase, PTEN (phosphatase and tensin homolog deleted on chromosome 10), has been solved.³¹ PTEN has been shown to dephosphorylate tyrosine- and serine/threonine-phosphorylated peptides³² as well as inositol phospholipids such as PIP₃ (phosphatidylinositol-3,4,5-triphosphate).³³ It is now

generally believed that PTEN is a bona fide phospholipid phosphatase and not a protein phosphatase. PIP₃ is an important second messenger involved in signaling during cell growth.³⁴ PTEN has been proposed to act as a tumor suppressor, suppressing both cell proliferation and growth by negatively controlling the phosphoinositide 3-kinase signaling pathway.^{35–37} While PTEN shows no significant sequence homology with any of the dual-specificity PTPs other than the active-site signature C(X)₅R, the phosphatase domain of PTEN shows a high degree of structural similarity to VHR (Figures 1 and 3). The active-site cleft of PTEN is noticeably larger than VHR or PTP-1B, however. The cleft is twice as wide but similar in depth to PTP-1B. With respect to VHR, the active-site cleft is both wider and deeper. Also, the signature motif of PTEN is highly basic in nature, which has led Lee and co-workers to propose how PTEN might bind PIP₃.³⁸ Recent work involving the disruption of PTEN in mice and in the worm *Caenorhabditis elegans* as well as the expression of PTEN in tumor cells containing nonfunctional PTEN alleles provides even stronger support for the idea that in vivo PTEN acts as a lipid phosphatase.³⁹

2. Low Molecular Weight Phosphatases

A number of low molecular weight protein tyrosine phosphatases (LMW-PTPs) have been isolated and their corresponding crystal structures solved from a variety of sources including human,⁴⁰ bovine,^{41–43} and yeast.⁴⁴ While the in vivo functions of these phosphatases is not yet well-defined, they have been shown to dephosphorylate phosphotyrosine-containing substrates.^{45–47} In addition, overexpression of a bovine liver LMW-PTPs in normal and transformed cells has been shown to inhibit cell proliferation.^{48,49} With the exception of the active-site sequence C(X)₅R-

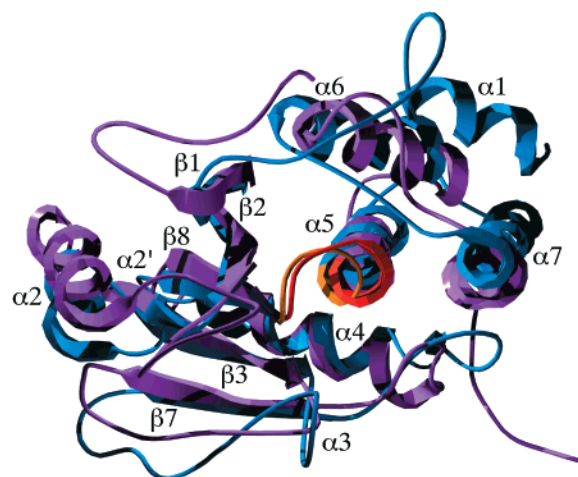


Figure 3. Ribbon diagrams of VHR (blue) and PTEN (purple) superimposed to show the structural similarity between the two phosphatases. The phosphate-binding loop for VHR is highlighted in gold, while the phosphate-binding loop for PTEN is in red. Ribbon diagrams of VHR and PTEN were obtained from the crystal structures published by Yuvaniyama et al.¹⁸ and Lee et al.,³¹ respectively. The nomenclature is that published for VHR by Yuvaniyama et al.¹⁸ Structures were generated using Swiss Pdb Viewer v3.5²³ and POV-Ray v3.1.

(S/T), LMW-PTPs share no sequence homology with other PTPs, either receptor-like (LAR and RPTP α) or nonreceptor-like (PTP-1B, VHR, Cdc25).⁴³ As illustrated in Figure 1, the topology of the LMW-PTPs is even divergent from the larger PTPs. Like the PTPs, LMW-PTPs contain a conserved aspartate residue, which is also required for activity.³⁰ The presence of the conserved arginine, aspartic acid, and cysteine residues within all LMW-PTPs is similar to that observed with the PTPs and suggests that a common catalytic mechanism is employed by both protein phosphatase families.

3. Cdc25

In 1998, Fauman and co-workers reported the first crystal structure of the catalytic domain of human Cdc25A.⁵⁰ The human Cdc25 family of phosphatases (Cdc25A, Cdc25B, and Cdc25C) appears to regulate progression of cells through the cell cycle by dephosphorylating specific Cdc2/Cyclin complexes.^{51–54} Cdc25 functions to dephosphorylate the cyclin-dependent kinase Cdc2 in the fission yeast *Schizosaccharomyces pombe*.^{55–57} As illustrated by Figure 1, the topography of Cdc25A is dramatically different from the other known PTPs, suggesting that the Cdc25 phosphatases represent a unique family. Although the Cdc25 phosphatases contain the recognized C(X)₅R signature motif, they do not share sequence homology with the catalytic domains of any protein phosphatases.⁵⁸ The folding pattern of Cdc25A is, however, similar to that of a bacterial rhodanese from *Azotobacter vinelandii*.⁵⁹ While rhodanese catalyzes the transfer of sulfane sulfur from thiosulfate to cyanide, generating thiocyanate and sulfite (Figure 4), the exact biological role of this enzyme remains to be determined. Rhodanese contains a nucleophilic cysteine residue which forms an initial persulfite linkage (R–S–S[–], Figure 4).⁶⁰ A number of cationic residues

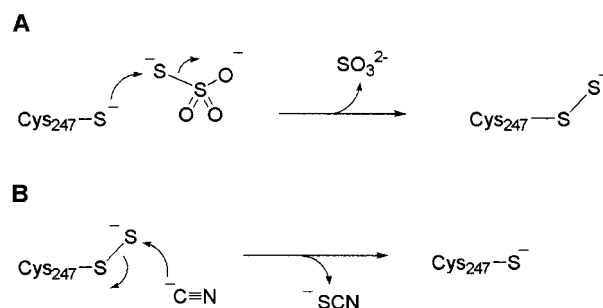


Figure 4. (A) Generalized mechanism for the formation of the initial persulfite linkage from thiosulfate and rhodanese. Cysteine numbering is for mammalian mitochondrial rhodanese. (B) Cleavage of the persulfite linkage by cyanide to regenerate the active-site cysteine nucleophile and thiocyanate.

lining one side of the active site, including Arg-186, are believed to position the thiosulfate residue as well as polarize the S–S bond in thiosulfate for nucleophilic attack by the catalytic cysteine residue.⁶¹ In the presence of a suitable nucleophile such as cyanide, the persulfite linkage is cleaved to regenerate the active form of the enzyme and thiocyanate.

On the basis of the presence of the C(X)₅R motif in Cdc25 phosphatases, a mechanism similar to that of the PTPs and LMW-PTPs has been proposed based upon kinetic studies using Cdc25A.⁶² However, the catalytic domain of Cdc25A does not adopt a similar conformation to the PTPs nor does it appear to bind oxyanions,⁵⁰ which has led some to propose that the catalytic mechanism used by Cdc25A is more closely related to rhodanese than PTPs.⁶³

Recently, the crystal structure of the catalytic domain of Cdc25B was reported.⁶⁴ A comparison of the structure of Cdc25B to that of Cdc25A⁵⁰ revealed similarity within the catalytic domain. Interestingly, key differences in the position of residues believed to be essential for catalysis between Cdc25A and Cdc25B were observed. For example, the carbonyl group of residue 434 in Cdc25A (residue 477 in Cdc25B) points toward the location where phosphate should bind, which is opposite for that observed with Cdc25B and other PTPs.^{18,21} Also observed was a difference in the positioning of the side chain for Arg-436 in Cdc25A. In Cdc25B, the corresponding arginine residue at position 479 forms a hydrogen bond with Glu-431, which is comparable to that observed with other PTPs. Cdc25B also contains the C(X)₅R motif and was found to bind tungstate and sulfate ions⁶⁴ in a conformation similar to that observed with other PTPs.^{18,21} Deletion of the C-terminal residues in the catalytic domain of Cdc25B (up to the location where both Cdc25A and Cdc25B deviate in structure) resulted in nearly a 10-fold decrease in apparent binding affinity for *p*NPP, indicating that the C-terminal region in Cdc25B may be required for substrate binding.⁶⁴

B. Important Sequences Outside the Catalytic Domain and Substrate Specificity of PTPs

The overall sequence identity and quaternary structure of protein tyrosine phosphatases varies greatly from family to family. Additional domains

important for the biological function of the enzyme may include amino-terminal immunoglobulin domains followed by fibronectin-type repeats such as that found in the receptor-type PTPs (RPTPs).¹¹ The RPTPs have been proposed to function in the regulation of cell–cell contact and adhesion through homophilic binding interactions between adjacent cells.^{66–69} The RPTPs contain either one or two intracellular domains (D1, membrane–proximal domain; D2, membrane–distal domain) responsible for phosphatase activity. Interestingly, for those PTPs that contain two catalytic domains, D1 but not D2 domains exhibit efficient catalytic activity for several RPTPs including RPTP α , CD45, and CLR-1.^{70–72} The D2 domains of RPTP γ and RPTP ζ lack the cysteine nucleophile, and most D2 domains do not contain the general-acid aspartate.^{73,74} Additional mutations in the primary structure of D2 from RPTP α (specifically at positions 555 and 690 which reside in the general-acid loop of D2, respectively) have recently been identified and may explain the lack of activity of domain D2.⁷⁵ While the function of the D2 domain remains to be determined, it is highly conserved among the RPTPs, suggesting an important role.

Some PTPs contain SH2 domains, such as those observed in SHP-2. SH2 domains are binding sites for phosphotyrosine-containing peptides and consist of approximately 100 residues. SHP-2 has been proposed to participate in signaling cascades initiated from receptor-mediated activation of Ras.¹⁰ Subcellular targeting domains, located on the C-terminal segment of many intracellular PTPs, are thought to help direct the PTP to specific locations within the cell and may also play a role in substrate specificity. Several of the DS–PTPs contain two N-terminal CH2 (Cdc25 homology 1 or 2) motifs which display limited similarity to the putative catalytic domains of Cdc25 phosphatases.^{76,77} The N-terminal noncatalytic region of the DS–PTP MKP-3 (mitogen-activated protein kinase phosphatase-3) displays tight binding toward its substrate, ERK (extracellular signal-regulated kinase). The DS–PTP M3–6, which has a similar N-terminal noncatalytic region, shows specific inactivation of both ERK and SAPK/JNK MAP kinases.^{78–80} Chimeras between MKP-3 and M3-6 have suggested that the N-terminal domain may be a key component in selectively dephosphorylating the ERK family of MAP kinases.⁸⁰

The specificity of PTPs toward phosphorylated substrates has been examined with a number of phosphatases and, in many respects, cannot be isolated to a single structural feature. As mentioned previously, the increased specificity of PTPs such as PTP-1B and *Yersinia* PTP toward phosphotyrosine-containing substrates can, in part, be due to the depth of the active-site cleft. Jia and co-workers have shown that amino acid residues YRDV(46–49) located between the first β -strand and first α -helix in PTP-1B make specific contacts to the peptide backbone and the phosphotyrosine ring of the substrate.⁸¹ This four amino acid sequence contributes to the overall depth of the pocket. As observed with VHR, the loop connecting α 1 and β 1 is about 75% shorter than PTP-1B, resulting in an active-site cleft that is



Figure 5. Ribbon diagram of human LMW–PTP with HEPES complexed in the active site. The variable loop is in blue, and the active-site signature motif CXXGXXR–(S/T) is in purple. The location of residues 49, 50, and 53, which are believed to participate in substrate specificity, are located in red. The diagram was generated from the crystal structure of human LMW–PTP published by Zhang et al.⁴⁰ The structure was generated using Swiss Pdb Viewer v3.5²³ and POV–Ray v3.1.

not as deep as that observed in the PTPs. This might explain the broader phosphatase activity toward phosphoserine/phosphothreonine-containing peptides.¹⁸ This decreased active-site depth of VHR allows for the dephosphorylation of many substituted aromatic phosphoesters which are inadequate substrates for PTPs, based upon steric effects of substituents on the aromatic ring.⁸²

Residues residing in the catalytic domain of many PTPs have been implicated in the specificity of substrates. Keilhack and co-workers proposed that the specificity of the catalytic domains toward epidermal growth factor receptor by SHP-1 and SHP-2 is responsible for substrate specificity and not the SH2 domains.⁸³ Similar conclusions have been proposed by O'Reilly and co-workers based upon studies on the influence of SHP-1 and SHP-2 on *Xenopus* oocyte maturation.⁸⁴ Moreover, substrate trapping mutants of PTP-1B have shown selective substrate recognition that appears to be mediated by the catalytic domains.^{85,86} A variable region (referred to as the variable loop) in the human low molecular weight PTP isozymes HCPTPA and HCPTPB (residues 40–73 using LMW–PTPs numbering, Figure 5) has been proposed to account for the differences in substrate specificity of these enzymes as well.⁴⁰ The variable loop comprises the floor and one wall of a long crevice that leads away from the active site in LMW–PTPs. A comparison of the X-ray crystal structure of a human LMW–PTP to that of bovine LMW–PTP (BPTP) has suggested that residues Trp-49, Asn-50, and Arg-53 (bovine LMW) and Tyr-49, Glu-50, and Asn-53 (human LMW–PTP), which are positioned along the long crevice leading away from the active site, are responsible for the observed substrate specificity between the two phosphatases.⁴⁰

It has been demonstrated that PTP-1B shows a preference for acidic and hydrophobic peptides by using the undecapeptide DADEpYLIPQQG (EGFR-

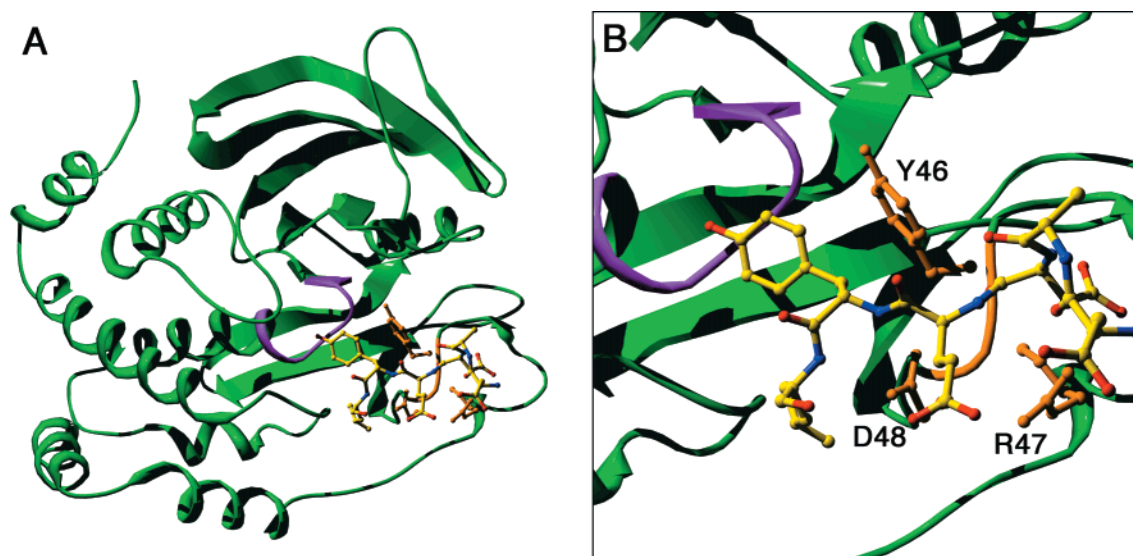


Figure 6. Ribbon diagram of (A) the PTP-1B mutant C215S complexed with the peptide DADEpYL-NH₂ and (B) on expanded view showing the position of specific residues relative to the peptide. For the peptide, the color yellow represents carbon atoms, red represents oxygen atoms, and blue represents nitrogen atoms. The active-site signature motif CXXGXXR-(S/T) is in purple. The locations of residues Tyr-46, Arg-47, and Asp-48, which are believed to participate in substrate specificity, are located in orange. The diagram was generated from the crystal structure of the PTP-1B mutant C215S complexed with the peptide DADEpYL-NH₂ published by Jia et al.⁸¹ The structure was generated using Swiss Pdb Viewer v3.5²³ and POV-Ray v3.1.

(988–998) as a model.^{87,88} EGFR(988–998) (epidermal growth factor receptor, residues 988–998) has been shown to be an excellent substrate for PTP-1B. These observations have also been supported using an “inverse alanine scanning” technique.⁸⁹ In this approach, the substitution of a single alanine for one of the 19 non-alanine residues in the peptide Ac-AAAAPYAAAA-NH₂ generates a library containing 153 specific peptides. The resulting peptides are then analyzed for their effect upon substrate binding and catalysis. From their results, Vetter et al. not only supported the initial observations reported by Zhang et al.,^{87,88} but also observed a preference for lysine and arginine residues at any position of the peptide substrate. Additional results suggested that residues at the +1 position (with respect to phosphotyrosine) may also contribute to substrate specificity.

Using the PTP-1B mutant C215S complexed with DADEpYL-NH₂ as well as site-directed mutants of PTP-1B (Tyr-46, Arg-47, Asp-48, Phe-182, and Gln-262), amino acids residing near the catalytic cleft have been suggested to play a part in substrate recognition and specificity, specifically Tyr-46, Arg-47, and Asp-48 (Figure 6).^{81,90} To explain the preference for acidic, aliphatic, or aromatic substrates, crystal structures of the mutant PTP-1B-(C215S) complexed with Ac-ELEFPYMDYE-NH₂ and Ac-DAD(Bpa)pYLIPQQG-NH₂ (Bpa, *p*-benzoylphenylalanine) were obtained.⁹¹ From the analysis of the crystal structures of the PTP-1B mutant complexed with either peptide, it was observed that Arg-47 forms two different conformations, depending on the substrate. For acidic residues at -1 and -2 (in relation to phosphotyrosine in the peptide substrate), Arg-47 adopts a conformation allowing hydrogen bonds to the carboxylate residues in the substrate. When the residue at -1 is aromatic or aliphatic, Arg-47 adopts a different conformation so the meth-

ylene carbons in the side chain can participate in hydrophobic interactions.

Recently, Peters and co-workers identified a key residue which appears to impart substrate specificity to the PTPs PTP-1B and PTP α .⁹² The peptide Ac-DADE(pY)L-NH₂ as well as several analogues of Ac-DADE(pY)L-NH₂ were used to identify position 259 (Gly-259, PTP-1B numbering) as a key determinant in substrate specificity. Ac-DADE(pY)L-NH₂ is derived from the epidermal growth factor receptor and shows a higher degree of recognition by PTP-1B as substrate in comparison to PTP α . In PTP-1B, a glycine resides at position 259, which is proposed to account for its broader substrate recognition. In PTP α , glutamine is at position 259, which causes steric hindrance due to the larger side chain and results in further substrate discrimination. Further studies using inhibitors of PTPs and X-ray crystallography suggested that Gln-259 might also play a role in catalysis by positioning the important residue Gln-262. Gln-262 is believed to be important in substrate binding, enzyme–phosphate (E–P) formation, and E–P hydrolysis.⁹⁰

The DS-PTPs MKP-3 and VHR show a preference for diphosphorylated substrates. Using diphosphorylated MAP(177–189) kinase (DHTGFLpTEpYVATR) and JNK1(180–189) kinase (FMMpTPpYVVTR), Denu et al. observed that diphosphorylated substrates are the best substrates in terms of phosphotyrosine hydrolysis ($K_m = 100\text{--}200\ \mu\text{M}$ and $V/K = 30\ 000\ \text{M}^{-1}\ \text{s}^{-1}$, where K_m is the Michaelis–Menton binding constant and V/K represents the apparent second-order rate constant).⁹³ As compared to diphosphorylated peptides, peptides monophosphorylated on tyrosine had K_m values of greater than 1.0 mM. VHR was shown to hydrolyze tyrosine first at a rate of $30\ 000\ \text{M}^{-1}\ \text{s}^{-1}$ followed by slower hydrolysis ($15\ \text{M}^{-1}\ \text{s}^{-1}$) at the threonine position. A conserved

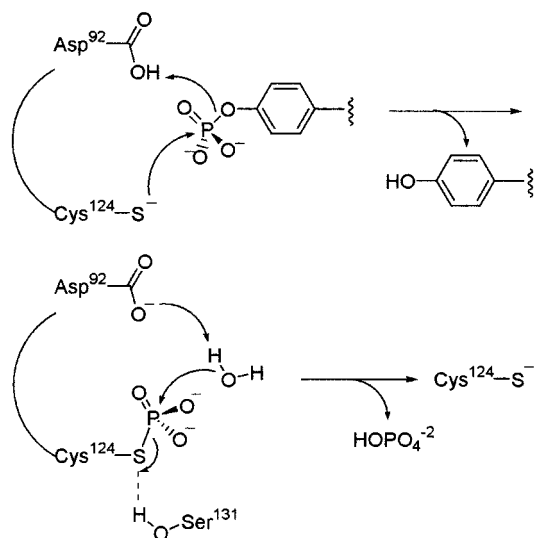


Figure 7. Common mechanism employed by PTPs using VHR numbering of many important amino acid residues involved in catalysis.

arginine residue (Arg-158) resides on the surface of the enzyme and is in close proximity to the active site. Arginine residues have been proposed as anion recognition sites in enzymes⁹⁴ and, therefore, may be the binding site for the second phosphorylated residue in the substrate. This anion (phosphate) recognition site may also be important in substrate specificity for VHR and other DS-PTPs whose protein substrates are diphosphorylated.

Crystallographic, peptide-binding studies, and kinetic data have shown that PTP-1B prefers tandem diphosphorylated substrates. PTP-1B has been implicated in the regulation of insulin receptor signaling.⁹⁵ Using the insulin receptor kinase (IRK) activation segment, Salmeen et al. observed specific interactions between the phosphorylated residues Tyr-1162 and Tyr-1163 and PTP-1B.⁹⁶ Residue Tyr-1162 was identified as the residue targeted by PTP-1B for hydrolysis, while residue Tyr-1163 is located in close proximity to a phosphotyrosine-binding site. PTP-1B exhibited K_m values for monophosphorylated peptides that were 10-fold higher than the K_m values for tandem diphosphorylated peptides. Peptide-binding studies also showed a 70-fold greater affinity for the tandem phosphorylated peptide.

C. Catalytic Mechanism of Protein Tyrosine Phosphatases

1. Role of the Conserved Cysteine, Arginine, and Aspartate Residues

Over the last several years, a substantial amount of research has clarified much of the mystery behind catalysis of the protein tyrosine phosphatases. In the dephosphorylation of protein substrates, two chemical steps are required as depicted in Figure 7. The first enzymatic step results in the formation of a transient enzyme-phosphate intermediate and release of the product via nucleophilic attack of the catalytic cysteine thiolate. The second enzymatic step requires hydrolysis of the enzyme-phosphate intermediate to generate inorganic phosphate and the

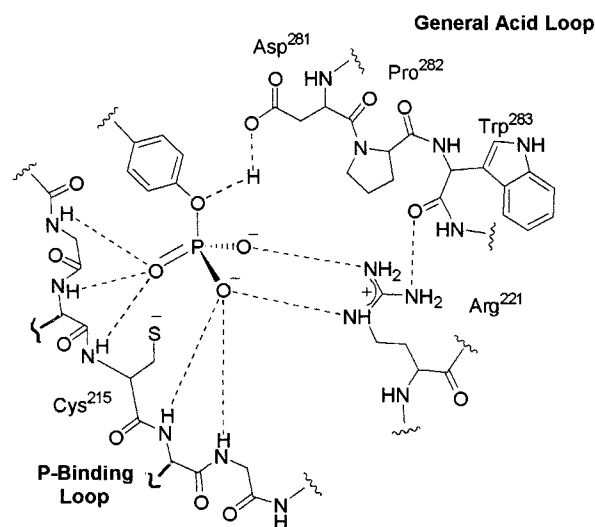


Figure 8. Schematic view of the hydrogen-bonding network in the active sites of PTPs (using PTP-1B numbering) showing both interactions between substrate and the peptide backbone of the phosphate-binding loop as well as interactions with the general-acid loop.

regenerated enzyme. The conserved cysteine residue has been shown to be essential in all PTP families such as the dual-specificity PTP VHR,²⁴ the receptor-like PTPs CD45, LAR, and RPTP μ ,⁹⁷⁻⁹⁹ the PTP PTP1,¹⁰⁰ and LMW-PTPs.²⁶ The pK_a value of a typical cysteine within a peptide or protein is approximately 8.5. The active-site cysteine in PTPs, however, has a very low pK_a and ranges from approximately 4.7 as reported in *Yersinia* PTP¹⁰¹ to 5.5 in VHR.²⁸ In the *Yersinia* PTP, a histidine residue at position 402 has been hypothesized to decrease the pK_a of the active-site cysteine (Cys403) by 2.7 pH units,¹⁰¹ while threonine at position 410 lowers the pK_a of Cys403 by 0.6 pH units.¹⁰² Histidine does not directly hydrogen bond to cysteine but instead participates in a network of hydrogen bonds that effectively polarizes the amide N-H groups in the backbone of the phosphate-binding loop and provides positive microdipoles which are oriented toward the cysteine residue.^{21,22,103} Zhang and Dixon demonstrated that if the histidine residue in *Yersinia* PTP (His402) is substituted with asparagine (Asn) or alanine (Ala), the pK_a of the active-site cysteine increases to 5.99 and 7.35, respectively.¹⁰¹ This effect is most likely due to the disruption of the hydrogen-bond network within the active site. The low pK_a of the conserved cysteine ensures that it is deprotonated and in the thiolate form at physiological conditions.

Upon substrate binding, several ionic interactions between the phosphate residue and the active site are formed. The conserved active-site arginine residue coordinates with two of the oxygen atoms on the phosphoryl group via its guanidinium side chain (Figure 8).^{18,21,43,44,81} If the arginine is replaced with lysine or alanine, these interactions are disrupted and an approximately 30-fold increase in K_m and an approximately 8000-fold decrease in k_{cat} was observed.²⁵ The remaining nonbridged oxygen atom points toward the backbone amides of the phosphate-binding loop.

After substrate binding, the nucleophilic cysteine thiolate reacts with the phosphorylated tyrosine, serine, or threonine residue to form an initial thiophosphate intermediate and dephosphorylated product (Figure 7). The conserved cysteine residue is located at the base of the active-site cleft and is positioned directly beneath the phosphate group of the substrate (Figures 2 and 8). The substrate is situated such that nucleophilic attack by the cysteine thiolate is in line with the P–O bond, which would allow for expedient expulsion of the leaving group from the active site. Evidence of the formation of the thiophosphate intermediate has been obtained through the use of ^{32}P -labeled substrates and ^{31}P NMR^{24,100,104,105} as well as through the analysis of the X-ray crystal structure of the Gln262Ala mutant of PTP-1B.¹⁰⁶

A conserved aspartic acid residue is positioned near the top of the cleft on a flexible loop (general-acid loop) and is thought to not only play a role in the formation of the thiophosphate intermediate, but also participate in the hydrolysis step to regenerate the enzyme (Figure 7).^{104,107} Site-directed mutagenesis of the aspartic acid residue and pH rate profile experiments have confirmed the involvement of this residue in catalysis.^{28–30,107} Crystallographic data from the thiophosphate intermediate of the PTP-1B mutant PTP-1B(Gln262A)¹⁰⁶ and *Yersinia* PTP complexed with tungstate²¹ has shown that upon substrate binding movement in the general-acid loop (approximately 6 Å) occurs, bringing the aspartic acid residue closer to the active site and in position to act as a general acid/base. The guanidinium group of the conserved arginine residue within the phosphate-binding motif makes an additional hydrogen bond to a peptide backbone carbonyl three residues away from the general-acid aspartate (Figure 8).^{18,21,43,44,81} Upon protonation and departure of the leaving group, the resulting aspartate residue hydrogen bonds to a water molecule, activating the water molecule for hydrolysis of the thiophosphate.¹⁰⁴ The role of aspartate as a general acid/base may not be applicable to all PTPs, however. Fauman et al.⁵⁰ theorized that the corresponding aspartic acid residue in Cdc25A (Asp-383), which was initially proposed as the general acid,¹⁰⁸ may serve more of a structural role and that Glu-431, which is the first X residue in the HCXXGXXR signature motif for Cdc25A, may play the role of general acid. From the crystal structure of Cdc25A, it was determined that Asp-383 is positioned away from the active site and forms a hydrogen bond with Arg-385, making the aspartic acid residue unavailable for protonation of the leaving group or hydrolysis of the enzyme–phosphate intermediate.

Recently, Chen et al. showed that the location of the general-acid residue required for catalysis by Cdc25B does not reside within the known structure of Cdc25B but may be located on its protein substrate, Cdk2.⁶⁵ Mutating the residues Glu-474 or Glu-478 of Cdc25B to glutamine, which lie in close proximity to the active site, exhibited no effect on the catalytic activity in comparison to wild-type Cdc25B when using *p*NPP as substrate. When the natural

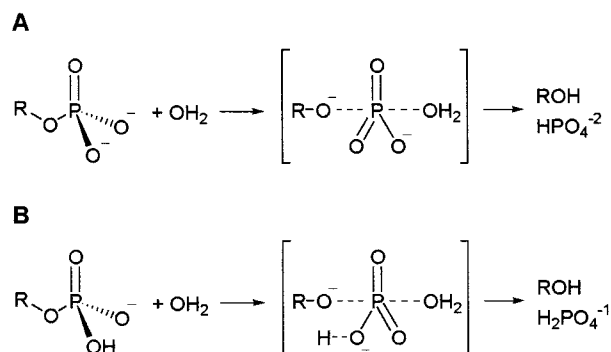


Figure 9. Reaction and transition-state structures of phosphate monoester (A) dianions and (B) monoanion in aqueous solutions.

substrate Cdk2-pTpY-Cyclin A was used, however, the E474Q mutant was 100-fold less active than wild-type. Because Glu-474 is conserved among all known Cdc25 phosphatases, the authors concluded that Glu-474 may be required for substrate recognition. When the pH profiles of wild-type Cdc25B using *p*NPP or MFP (3-*O*-methylfluorescein phosphate) were compared to the pH profile of wild-type Cdc25B using the natural substrate Cdk2-pTpY/Cyclin A, striking differences were observed. A typical pH profile for the PTPs and DS-PTPs shows a pH dependency below 4–6 as well as a pH dependency above pH 6–7. The cysteine nucleophile is responsible for the critical ionization below pH 6 and must be unprotonated for activity. The conserved aspartic acid residue is responsible for the ionization above pH 7 and must be protonated for maximal activity. The pH profiles using *p*NPP or MFP as substrate for Cdc25B showed a lack of pH dependence above pH 6.5, indicating the absence of a general-acid residue.⁶⁵ The pH profile using Cdk2-pTpY/CycA, however, showed a substantial decrease in V/K as pH increased above pH 6.5, indicating that a residue required protonation for optimal activity of wild-type Cdc25B. The latter pH profiles for the E474Q and E478Q mutants showed identical pH dependencies at higher pH in comparison to the wt-Cdc25B/Cdk2-pTpY/CycA pH profile, indicating that the mutations at Glu-474 and Glu-478 were not responsible for the ionization observed. These data provide support for the authors conclusion that the general acid required for activity may reside on the peptide substrate. The identity of possible glutamate or aspartate residues on the peptide substrate surface, however, has not been addressed.

2. Transition-State Structure and the Role of the Conserved Serine/Threonine Residue in Catalysis

The use of heavy-atom kinetic isotope effects has provided tremendous insight into the catalytic mechanism employed by the protein tyrosine phosphatases and phosphate transfer in general. There is strong evidence that phosphate monoesters in aqueous solution react as either monoanions or dianions by a dissociative mechanism^{109–113} in which the phosphorus atom in the transition state resembles metaphosphate (Figure 9). The dashed lines present in Figure 9 represent low bond order (<0.1) in the transition

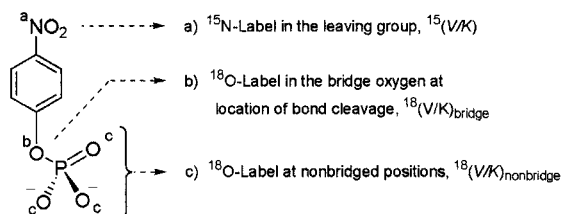


Figure 10. *p*-Nitrophenyl phosphate used for kinetic isotope studies described in this review, indicating the location and type of label used for measurements.

state, with advanced bond cleavage to the leaving group and minimal bond formation to the nucleophile. For the monoanions of phosphate monoesters, a dissociative mechanism in the transition state similar to dianions is proposed (Figure 9) but the proton is believed to be largely or totally shifted to the leaving group in the transition state.

By using *p*-nitrophenyl phosphate (*p*NPP) labeled at various positions with either ^{18}O or ^{15}N , three different kinetic isotope effects can be observed to examine the transition state of an enzymatic reaction in detail as illustrated in Figure 10. Primary ^{18}O isotope effects ($^{18}k_{\text{bridge}}$) provide a reliable indication of the degree of transition-state bond cleavage of the bridged oxygen atom. Secondary ^{18}O isotope effects ($^{18}k_{\text{nonbridge}}$) are observed in the nonbridged oxygen atoms and probe the changes in bond order that occur in the phosphoryl group. The magnitude of $^{18}k_{\text{nonbridge}}$ reveals whether the transition state goes through a dissociative mechanism (metaphosphate-like, Figure 9) or an associative mechanism, similar to a pentavalent phosphorane. By placing ^{15}N in the nitro group of *p*NPP, the ^{15}N isotope effect (^{15}k) measures the extent of charge delocalization into the phenyl ring of the leaving group. The primary, secondary, and ^{15}N isotope effects for the nonenzymatic hydrolysis of both the monoanion and dianion of *p*NPP in solution have been reported and are consistent with a dissociative transition state for the nonenzymatic hydrolysis of phosphate monoesters.¹¹⁴ It has been proposed, however, that enzymatic hydrolysis of phosphate monoesters should proceed more through an associative mechanism because the side chains in the active site of the enzyme should be able to stabilize the developing negative charge on the phosphoryl group in the transition state.^{115,116} In 1995, Han and Coleman proposed that the transfer of phosphate from phosphorylated substrates to a nucleophilic cysteine residue in an alkaline phosphatase mutant proceeded through an associative mechanism with decreased bond cleavage to the leaving group.¹¹⁷

p-Nitrophenyl phosphate has been shown to be a good substrate analogue for the PTPs, and as a result, kinetic isotope studies have been performed to probe the mechanism. For these enzymatic reactions, isotope effects are manifested in V/K and provide information on the chemical step of phosphoryl transfer from substrate to the nucleophilic cysteine residue. In 1995, Hengge and co-workers reported the first kinetic isotope studies on PTPs using *Yersinia* PTP and PTP1 from rat.¹¹⁸ Table 1 lists the results from the kinetic isotope study as well

as for the hydrolysis of *p*NPP in solution. The magnitudes of the $^{18}(V/K)_{\text{bridge}}$ (Figure 10) isotope effects were similar to those measured in solution, indicating that the chemical step is rate-limiting for V/K and that the transition state proceeds through a dissociative-like mechanism. This suggests that binding of substrate as well as the conformational change induced upon binding of substrate²¹ was rapid and reversible. If these steps were partially or fully rate-limiting, the magnitude of the isotope effects would be suppressed. The cleavage of the P–O bond in the substrate is well advanced with very little bond formation to the nucleophilic cysteine. The similarity of the $^{18}(V/K)_{\text{nonbridge}}$ isotope effects between the enzymatic and nonenzymatic reaction for the dianion (Table 1) suggests that the phosphorus atom adopts a metaphosphate-like structure in the transition state. The $^{15}(V/K)$ isotope effect for the enzymatic reactions was not observed. This indicated complete charge neutralization in the leaving group by the transfer of a proton from the conserved aspartic acid residue. This charge neutralization compensates for the cleavage of the P–O bond and buildup of negative charge in the transition state. Using the *Yersinia* PTP mutants D356A and D356N as well as the PTP1 mutant D181N, the role of the conserved aspartic acid residue in catalysis was further investigated. A substantial $^{15}(V/K)$ for all three mutants was observed (Table 1), indicating that the leaving group was departing as the *p*-nitrophenolate anion and that the aspartic acid residue was directly accountable for protonation of the leaving group with the native enzyme.

Kinetic isotope studies using the native DS–PTP VHR and with the mutants D92N and S131A and the double mutant D92N/S131A were also performed.¹¹⁹ The magnitudes of $^{15}(V/K)$, $^{18}(V/K)_{\text{bridge}}$, and $^{18}(V/K)_{\text{nonbridge}}$ for native VHR and mutant D92N (Table 1) were similar to those obtained with *Yersinia* PTP and rat PTP1 as well as the nonenzymatic reaction. In the transition state for VHR, substantial P–O bond cleavage and proton transfer from aspartic acid to the leaving group occurs. In addition, minor bond formation between the nucleophilic cysteine and the phosphate residue occurs in the transition state.

More recent kinetic isotope studies using the low molecular weight PTP Stp1 and with the mutants D128A, D128E, and D128N were performed to compare the transition state of LMW–PTPs with the other PTPs.¹²⁰ Stp1 has been shown to act as a multicopy suppressor of the cell cycle regulator *cdc25* temperature-sensitive mutants.¹²¹ The values for $^{15}(V/K)$ and $^{18}(V/K)_{\text{nonbridge}}$ (Table 1) using native Stp1 differed from those values measured using *Yersinia* PTP and VHR. The transition state still appeared to be highly dissociative with respect to P–O cleavage in the leaving group. Surprisingly, a larger $^{15}(V/K)$ effect was observed with respect to the $^{15}(V/K)$ values obtained for *Yersinia* PTP and VHR, indicating an increased negative charge on the leaving group in the transition state. A small decrease in the P–O bond order, as represented by $^{18}(V/K)_{\text{bridge}}$, was also observed relative to the $^{18}(V/K)_{\text{bridge}}$ values for *Yersinia* PTP and VHR. Hengge and co-workers proposed that

Table 1. Isotope Effects for Native and Mutant Enzymes of *Yersinia* PTP, PTP1, VHR, and Stp1 Using *p*NPP

enzyme	enzymatic reactions		
	$^{15}(V/K)$	$^{18}(V/K)_{\text{bridge}}$	$^{18}(V/K)_{\text{nonbridge}}$
native <i>Yersinia</i> PTP ^b	0.9999 ± 0.0003	1.0152 ± 0.0006	0.9998 ± 0.0013
<i>Yersinia</i> PTP-D356A ^b	1.0022 ± 0.0003	1.0274 ± 0.0008	1.0007 ± 0.0005
<i>Yersinia</i> PTP-D356N ^b	1.0024 ± 0.0005	1.0275 ± 0.0016	1.0022 ± 0.0005
<i>Yersinia</i> PTP-W354A ^b	1.0021 ± 0.0002	1.0310 ± 0.0005	1.0038 ± 0.0005
<i>Yersinia</i> PTP-W354F ^b	1.0013 ± 0.0002	1.0240 ± 0.0010	1.0015 ± 0.0008
<i>Yersinia</i> PTP-R409K ^b	1.0020 ± 0.0005	1.0273 ± 0.0003	1.0049 ± 0.0007
<i>Yersinia</i> PTP-R409A ^b	1.0012 ± 0.0003	1.0200 ± 0.0005	0.9990 ± 0.0007
native rat PTP1 ^b	1.0001 ± 0.0002	1.0142 ± 0.0004	0.9981 ± 0.0015
rat PTP2-D181N ^b	1.0019 ± 0.0002	1.0278 ± 0.0017	1.0018 ± 0.0003
native VHR ^c	0.9999 ± 0.0004	1.0118 ± 0.0020	1.0003 ± 0.0003
VHR-D92N ^c	1.0030 ± 0.0002	1.0294 ± 0.0009	1.0019 ± 0.0005
VHR-S131A ^c	1.0002 ± 0.0003	1.0119 ± 0.0005	1.0001 ± 0.0006
VHR-D92N/S131A ^c	1.0029 ± 0.0003	1.0306 ± 0.0010	1.0031 ± 0.0007
native Stp1 ^d	1.0007 ± 0.0001	1.0160 ± 0.0005	1.0018 ± 0.0003
Stp1-D128A ^d	1.0030 ± 0.0005	1.0297 ± 0.0009	1.0010 ± 0.0006
Stp1-D128E ^d	1.0006 ± 0.0002	1.0166 ± 0.0010	1.0013 ± 0.0003
Stp1-D128N ^d	1.0034 ± 0.0003	1.0282 ± 0.0012	1.0024 ± 0.0005
Stp1-S18A ^d	1.0010 ± 0.0002	1.0172 ± 0.0013	1.0024 ± 0.0005
	solution reactions ^a		
	^{15}k	$^{18}k_{\text{bridge}}$	$^{18}k_{\text{nonbridge}}$
monoanion in water	1.0005 ± 0.0002	1.0106 ± 0.0003	1.0224 ± 0.0005
dianion in water	1.0034 ± 0.0002	1.0230 ± 0.0005	0.9993 ± 0.0007
dianion in <i>tert</i> -butyl alcohol	1.0039 ± 0.0003	1.0202 ± 0.0008	0.9997 ± 0.0016

^a From Hengge, A. C.; Edens, W. A.; Elsing, H. *J. Am. Chem. Soc.* **1994**, *116*, 5045–5049. ^b From Hoff, R. C.; Hengge, A. C.; Wu, L.; Keng, Y.-F.; Zhang, Z.-Y. *Biochemistry* **2000**, *39*, 46–54. ^c From Hengge, A. C.; Denu, J. M.; Dixon, J. E. *Biochemistry* **1996**, *35*, 7084–7092. ^d From Hengge, A. C.; Zhao, Y.; Wu, L.; Zhang, Z.-Y. *Biochemistry* **1997**, *36*, 7928–7936

this decrease would most likely be the result of increased nucleophilic interactions of the cysteine residue with the phosphate. Substitution of glutamic acid for the aspartic acid residue at position 128 had no appreciable effect on the transition state as observed in $^{15}(V/K)$, $^{18}(V/K)_{\text{bridge}}$, and $^{18}(V/K)_{\text{nonbridge}}$, indicating that the mutation is not effecting the transition state. This mutation has shown a 17-fold decrease in phosphoryl transfer relative to wild-type Stp1, however.¹²² As the authors conclude, the difference in activity between the D128E mutant and native Stp1 may be a result of improper positioning of the acidic residue due to the addition of an extra methylene in the side chain. When aspartic acid was replaced by alanine or asparagine, a dramatic increase in $^{15}(V/K)$ was observed. This provided evidence that without the acidic aspartic acid residue at position 128, the leaving group departs as the *p*-nitrophenylate anion but still goes through a dissociative transition state.

The conserved serine/threonine residue that resides within the C(X)₅R(S/T) signature domain has been shown to play a role in catalysis and may be used in the hydrolysis of the thiophosphate intermediate. Substitution of alanine for serine in VHR results in a 100-fold decrease in k_{cat} but only a 2–4-fold reduction in $k_{\text{cat}}/K_{\text{m}}$.¹²³ As a result of this substitution, the rate-limiting step in catalysis was clearly hydrolysis of the thiophosphate intermediate. The pK_{a} of the cysteine residue exhibits little change upon substitution, and because $k_{\text{cat}}/K_{\text{m}}$ is affected only slightly, serine does not appear to play a role in the initial formation of the thiophosphate intermediate. Instead, the hydroxyl group may play a pivotal role in the hydrolysis of the thiophosphate intermediate to regenerate the enzyme. Structural analysis of VHR,

Yersinia PTP, and PTP-1B suggests that their respective hydroxyl groups are close enough to participate in a hydrogen bond with the catalytic cysteine.^{18,21,22} These conserved hydroxyl-bearing residues (serine or threonine) could hydrogen bond with the cysteine of the thiophosphate intermediate. As a result of hydrogen bonding, the developing negative charge on cysteine in the transition state would be partially stabilized, making the thiolate a better leaving group. Measurement of kinetic isotope effects using the VHR mutant S131A (Table 1) indicates that there is no appreciable change in the structure of the transition state.¹¹⁹ In the double mutant D92N/S131A, the isotope effects $^{15}(V/K)$ and $^{18}(V/K)_{\text{bridge}}$ also exhibit no profound change, indicating similar degrees of bond cleavage on phosphorus and development of negative charge on the leaving group. A larger $^{18}(V/K)_{\text{nonbridge}}$ in comparison to the mutant D92N is observed, however. This is an indication of a loss of P–O bond order in the transition state but was proposed as the result of the increased repulsion of negative charges between the nucleophilic cysteine residue and phosphorus. Similar results were observed with the Stp1 mutant S18A.¹²⁰ While it has yet to be determined, serine/threonine may assist in aligning the thiol–phosphate intermediate for hydrolysis by water.

Recently, the effects of general-acid catalysis by mutations at a conserved tryptophan (located in the general-acid loop) and arginine (located in the signature motif C(X)₅R(S/T)) residue within *Yersinia* PTP were reported using both steady-state kinetics and heavy-atom isotope effects. Trp-354 (*Yersinia* PTP numbering) is a highly conserved residue among the phosphotyrosine-specific protein phosphatases. Tryptophan, the general-acid aspartate, and proline

make up the WpD motif found in most tyrosine-specific PTPs.^{21,22,29} Initial kinetic studies using the *Yersinia* PTP mutants W354F and W354A have shown that the K_m value for *p*NPP binding was similar to the native enzyme.¹²⁴ The k_{cat} values for the W354F and W354A mutants were 200-fold and 480-fold lower, respectively, from that of the native enzyme. These mutants also showed a leaving group and pH dependency similar to what was observed with the general-acid mutant D356N. For the mutant W354A, the V/K kinetic isotope effects are similar to those observed for the D356N mutant (Table 1), indicating that protonation by Asp-356 has been eliminated by the mutation and that there is substantial negative charge development on the leaving group in the transition state.¹²⁵ In comparison, the (V/K) kinetic isotope values for the mutant W354F are intermediate between those of the W354A and D356N mutant (Table 1), indicating partial proton transfer in the transition state but not as developed as that observed with the native enzyme. These results, combined with the steady-state experiments, suggest that Trp-354 is essential in the proper movement of the flexible general-acid loop for catalysis by the conserved aspartic acid residue. The question should be raised, therefore, as to why phosphotyrosine-specific PTPs require tryptophan two positions upstream of the general acid. The DS-PTPs do not have this conserved WpD motif. For example, VHR contains an alanine (Ala-90) in the same position as the tryptophan residue in *Yersinia* PTP,¹⁸ while MKP-3 contains an isoleucine (Ile-260 in MKP-3).¹²⁶ The isoleucine residue at position 260 in MKP-3 has also been proposed to interact with the guanidinium side chain of the conserved arginine residue at position 299 via the carbonyl backbone of isoleucine.¹²⁷ The presence of the tryptophan residue in PTPs, therefore, may be required to provide additional help in loop closure through π - π interactions between the phenyl ring of the substrate and the aromatic ring of tryptophan.

Mutations in the conserved arginine residues were also shown to effect catalysis. Interestingly, mutation of Arg-409 to lysine had a negligible effect on the K_m , but it is increased 30-fold in the Arg409Ala mutant, and the k_{cat} values for both mutants are about 4 orders of magnitude lower than those observed for the native enzyme.¹²⁵ The value of $^{15}(V/K)$ (Table 1) for the Arg409Ala mutant indicates partial proton transfer to the leaving group in the transition state, but general-acid catalysis is completely eliminated in the Arg409Lys mutant. The loss of catalytic activity that was observed in the Arg409Lys mutant could be a result of decreased hydrogen bonding to the oxygen atoms of phosphate in the transition state. A substitution for alanine at this position would eliminate all interactions between the phosphate oxygens and the guanidinium side chain of Arg-409. The effects of the Arg409Lys and Arg409Ala mutants on proton transfer in the transition state were more difficult to interpret by the authors, but they proposed that the observed effects may be a result of structural changes due to the addition of an extra methylene that is present in the side chain of lysine.

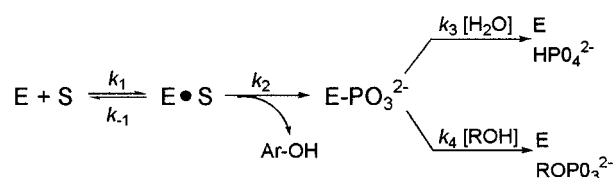


Figure 11.

This structural change may prevent movement in the general-acid loop, thus preventing Asp-356 from functioning as the general acid.

Using Stp1, the transition state for the hydrolysis of the thiophosphate intermediate has also been investigated.¹²⁸ In the presence of primary alcohols (methanol, ethanol, etc.), Stp1 has been shown to transfer phosphate to the alcohol in addition to the inorganic phosphate normally generated during the hydrolysis of aryl phosphates.^{129,130} This broad nucleophilic specificity in the hydrolysis of the thiophosphate intermediate has been utilized to obtain Brønsted β_{nu} values which may reflect the degree of bond formation between the nucleophile and the phosphorus atom in the transition state.¹³¹ The Brønsted β_{nu} parameter is obtained from correlation of reactivity as a function of the pK_a of the nucleophile. For the nonenzymatic hydrolysis of various phosphates with alcohols and amines, the β_{nu} value ranges between 0.10 and 0.14.^{132,133} Using various primary alcohols with pK_a values ranging from 12.4 to 16.1, the rates of hydrolysis (k_4) of the thiophosphate intermediate (Figure 11) were determined. A plot of $\log k_4$ versus the pK_a of the nucleophile provided a slope of $\beta_{nu} = 0.14 \pm 0.04$ and is in accord with the nonenzymatic hydrolysis of aryl phosphates with alcohols, suggesting that the transition state for hydrolysis of the thiophosphate intermediate is also highly dissociative. Using the Stp1 mutant S18A, a β_{nu} value of 0.26 ± 0.05 was obtained suggesting that the transition state has become less dissociative due to the increased negative charge that has developed on the nucleophile in the transition state. As a comparison, phosphate triesters react through an associative mechanism¹³⁴ and have β_{nu} values of 0.30–0.48.¹³⁵ The substitution of Ser-18 to alanine further supports the role of the conserved alcohol stabilizing the transition state during thiophosphate hydrolysis.¹⁰⁴

D. Regulatory Mechanisms of Protein Tyrosine Phosphatases

A universal mechanism for the regulation of phosphatase activity by PTPs has not been demonstrated. In general, PTP activity is not dependent upon posttranslational modification (e.g., acetylation, methylation, phosphorylation) because most recombinant PTPs expressed and purified from bacteria exhibit high catalytic efficiency. It is reasonable to propose, therefore, that catalytic activity is governed through negative regulation. In this section, three reversible regulatory mechanisms will be examined: regulation by intra- or intermolecular interactions, redox regulation of the catalytic cysteine residue, and phosphorylation of the protein tyrosine phosphatase.

Table 2. Isotope Effects for Native and Mutant MKP-3 in the Presence and Absence of ERK Using *p*NPP

enzyme	enzymatic reactions		
	$^{15}(V/K)$	$^{18}(V/K)_{\text{bridge}}$	$^{18}(V/K)_{\text{nonbridge}}$
MKP-3 with ERK	1.0004 ± 0.0001	1.0168 ± 0.0005	1.0006 ± 0.0003
MKP-3 without ERK	1.0008 ± 0.0001	1.0202 ± 0.0040	1.0012 ± 0.0005
MKP-3 mutant D262N w/ ERK	1.0031 ± 0.0004	1.0316 ± 0.0013	1.0023 ± 0.0006
MKP-3 mutant D262N w/o ERK	1.0027 ± 0.0004	1.0320 ± 0.0030	1.0023 ± 0.0006
	solution reactions ^a		
	^{15}k	$^{18}k_{\text{bridge}}$	$^{18}k_{\text{nonbridge}}$
monoanion in water	1.0005 ± 0.0002	1.0106 ± 0.0003	1.0224 ± 0.0005
dianion in water	1.0034 ± 0.0002	1.0230 ± 0.0005	0.9993 ± 0.0007
dianion in <i>tert</i> -butyl alcohol	1.0039 ± 0.0003	1.0202 ± 0.0008	0.9997 ± 0.0016

^a From Hengge, A. C.; Edens, W. A.; Elsing, H. *J. Am. Chem. Soc.* **1994**, *116*, 5045–5049. ^b From Rigas, R. D.; Hoff, R. H.; Rice, A. E.; Hengge, A. C.; Denu, J. M. *Biochemistry* **2001**, *40*, 4398.

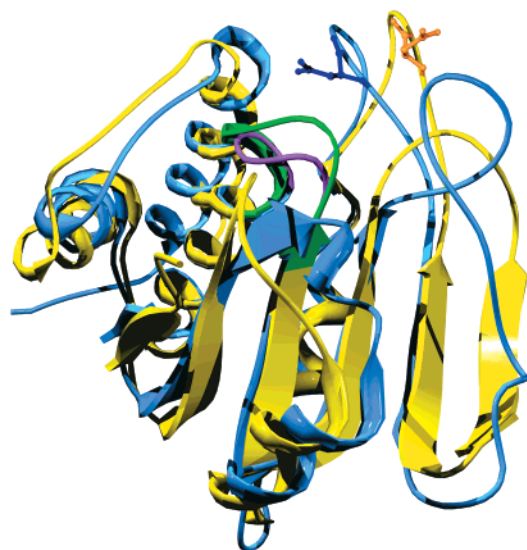


Figure 12. Ribbon diagrams of VHR (blue) and MKP-3 (yellow) superimposed to show the structural similarity between the two phosphatases. The phosphate-binding loop for VHR is highlighted in purple, while the phosphate-binding loop for MKP-3 is in green. The variable acid loop and location of the conserved aspartic acid residue for both phosphatases is labeled for clarity. Ribbon diagrams of VHR and MKP-3 were obtained from the crystal structures published by Yuvaniyama et al.¹⁸ and Stewart et al.,¹²⁶ respectively. Structures were generated using Swiss Pdb Viewer v3.5²³ and POV-Ray v3.1.

1. Regulation via Intra- or Intermolecular Interactions

The mitogen-activated protein kinase phosphatase 3 (MKP-3) is a dual-specificity PTP that shows a high degree of selectivity for ERKs over other MAP kinases such as c-Jun NH₂-terminal kinases/stress-activated protein kinases (JNK/SAPK) or p38 MAP kinases.^{78,79} MKP-3 was recently shown to be activated upon binding of ERK2 to its noncatalytic N-terminal domain.¹³⁶ Independently, both Denu¹²⁷ and Zhang¹³⁷ investigated the mechanistic basis for activation of MKP-3 by ERK2 and have come to similar conclusions. The recently published X-ray structure of the catalytic domain of Pyst1 (MKP-3)¹²⁶ revealed a structure that was similar to that of VHR.¹⁸ Surprisingly, the general-acid loop was flipped 20 Å away from the active-site cleft (Figure 12). Using a combination of Brønsted analysis and pre-steady-state and steady-state kinetics,^{127,137} both

groups presented data which supported a conformational change upon activation of MKP-3 by ERK2, bringing the general-acid Asp-262 close to the active site to participate in catalysis.

Although it had yet to be confirmed until recently, Rigas et al. identified Asp-262 as the general acid/base required for full catalytic activation of MKP-3 by ERK. Using wild-type MKP-3 and the MKP-3 mutant D262N, the kinetic isotope effects $^{18}(V/K)_{\text{bridge}}$, $^{18}(V/K)_{\text{nonbridge}}$, and $^{15}(V/K)$ (Table 2) were evaluated upon activation by ERK and the effect of the D262N mutation on the transition state.¹³⁸ From their results, the kinetic isotope effects were consistent with Asp-262 acting as general acid by protonating the leaving group. As expressed in the value for $^{15}(V/K)$ for the D262N mutant in comparison to wild type, the lack of the general acid results in the leaving group departing as the anion. Interestingly, substitution of aspartate for asparagine at position 262 did not totally eliminate activation by ERK. This residual activation of MKP3 mutant D262N by ERK may result from partial stabilization of the transition state for phospho–enzyme intermediate formation (4-fold) and increased phosphate affinity by approximately 8-fold. These results can best be explained by examining the influence of ERK upon the conformation of the general-acid loop. After binding to ERK, the general-acid loop of the mutant can still adopt the active closed conformation. This positions Arg-299 correctly within the active site by Ile-260 of the general-acid loop, stabilizing the phosphate oxygens during catalysis and substrate binding.

Recently, specific regions on ERK and MKP-3 have been identified which are important for binding and activation of MKP-3 by ERK. Nichols et al. identified specific subdomains within ERK2, using a series of p38/ERK chimeras, which are necessary for binding and catalytic activation of MKP-3.¹³⁹ Mutation of a kinase interaction motif (KIM) located at the N-terminus of MKP-3 resulted in loss of activation in the presence of ERK2. These results suggested that conserved residues found in the CH2 domain of MKP-3 are important for ERK2 binding. Using mutational and deletion experiments with MKP-3, Zhou et al. also identified regions on MKP-3 that are important for ERK binding and activation.¹⁴⁰ Specifically, deletion of the KIM motif (residues 61–75) resulted in a 125-fold reduction in ERK binding

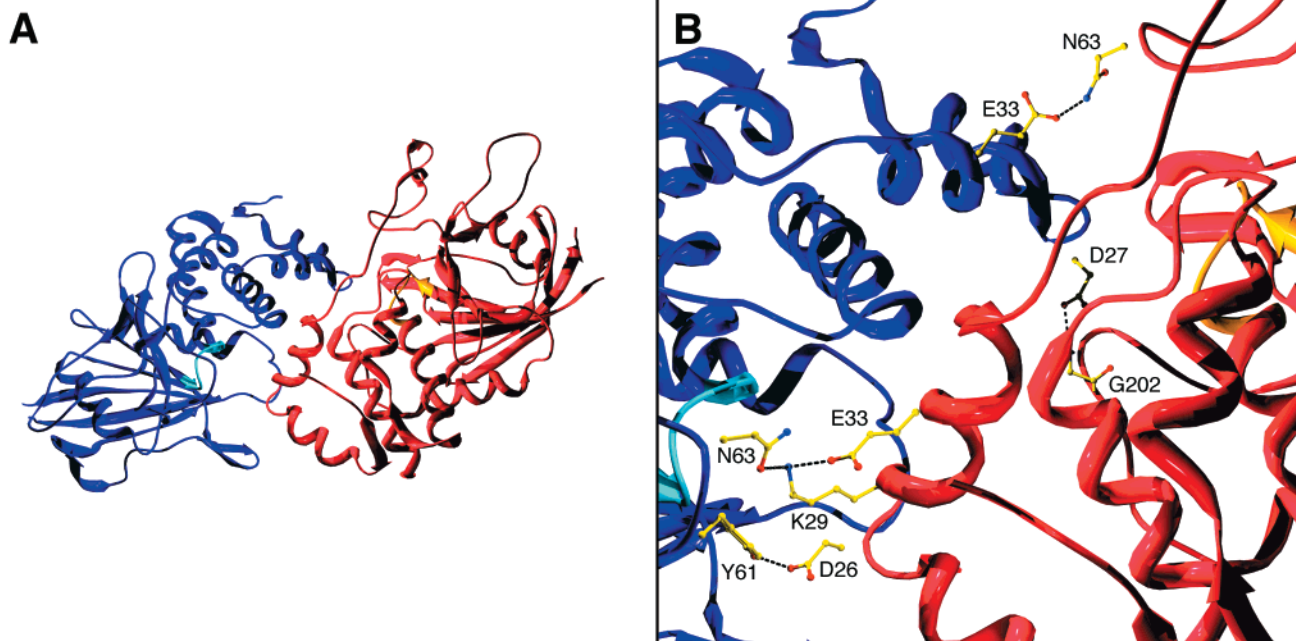


Figure 13. Ribbon diagram of (A) the RPTP α D1 dimer and (B) an expanded view showing hydrogen-bonding interactions (dotted black lines) between important residues in each monomer (blue and red). Carbon side chains are in yellow; nitrogen is represented as blue spheres and oxygen as red. The phosphate-binding loop for each monomer is highlighted in light blue and gold, respectively. The ribbon diagram was generated from the crystal of the RPTP α D1 dimer published by Bilwes et al.²⁰ using Swiss Pdb Viewer v3.5²³ and POV-Ray v3.1.

affinity while Arg-65 appears to be the most important residue in this region. A conserved sequence among all cytosolic MKPs (residues 161–177 in MKP-3) was also shown to effect ERK binding upon deletion, but the effect was substantially smaller (15-fold). A third sequence located in the C-terminal end of MKP-3 (residues 348–381) is believed to be important in activation. By examining the interactions between the N-terminal domain of MKP-3 and ERK in solution, Farooq et al. identified regions of the N-terminal domain that are important for MKP-3 activation.¹⁴¹ From their NMR solution structures and biochemical experiments, Farooq et al. identified regions essential to ERK binding that also made contacts to the C-terminal catalytic domain. Specific regions on the N-terminal domain of MKP-3 that interact with ERK were also shown to overlap with regions of contact between the N-terminal and C-terminal catalytic domain.

The N-terminal domain is a common characteristic among most of the MKPs, and specific binding and activation appears to be a general phenomenon of MKPs for their specific MAP kinases. While there is general agreement that binding of ERK2 to the N-terminal noncatalytic domain of MKP-3 induces a conformational change within the MKP-3/ERK2 complex, activating MKP-3 phosphatase activity, important questions remain unaddressed. Specifically, are all N-terminal noncatalytic domains involved in activation of the corresponding C-terminal catalytic domain? With respect to MKP-3, once MKP-3 is activated, does dephosphorylation occur on the ERK2 that is bound to MKP-3? Alternatively, does activated MKP-3/ERK2 dephosphorylate an additional ERK2 molecule? Also, is dephosphorylation ordered (e.g., pTyr first or pThr first) as well as processive? These questions can be and should be applied to other MKP

family members as well. These mechanistic questions will only be answered with further biochemical studies.

Upon publication of the X-ray structures of the D1 catalytic domains from RPTP α and RPTP μ , two distinct mechanisms have been proposed, even though the proteins share 46% sequence identity.^{20,142} With respect to RPTP α , an N-terminal helix–turn–helix was found to be inserted into the active site of a dyad-related D1 monomer (Figure 13).²⁰ This observation led Bilwes and co-workers to propose that dimerization of the D1 catalytic domain in RPTP α may be a method of regulation and might also be extended to other RPTPs as well. Additional support for the physiological importance of dimerization involved studies with the PTP CD45, which is required for T- and B-cell signaling.⁷¹ An EGF receptor-CD45 chimera containing the intracellular region of CD45 and the extracellular domain of the EGF receptor was introduced to cells that lacked CD45 function.¹⁴³ The enzyme activity of the EGF–CD45 chimera expressed in a T-cell line was inhibited by EGF-induced dimerization in a wedge-dependent manner and resulted in inhibition of T-cell signaling.^{143,144} Also, CD45 has been chemically cross-linked in lysates,¹⁴⁵ and the intracellular domain of CD45 has been shown to dimerize in solution,¹⁴⁶ illustrating the potential for dimerization by CD45. Support that RPTP α dimerization may occur in vivo was initially reported in 1999 by Jiang and co-workers.¹⁴⁷ Using the RPTP α mutant Pro137Cys (the location of position 137 resides in the extracellular domain), dimerization via a disulfide bond was observed, substantially reducing the biological activity. Recently, mutations in the wedge region of D1 and deletion of the entire D2 domain of RPTP α reduced but did not eliminate dimerization, suggesting that both domains are in-

involved in dimerization.¹⁴⁸ The transmembrane domain as well as the extracellular domain was also shown to dimerize, suggesting that interactions between all three domains (extracellular, transmembrane, and intracellular) may play an important role in regulating RPTP α activity in vivo.

With the publication on the X-ray crystal structure of the D1 catalytic domain of RPTP μ ¹⁴² however, homodimerization may not be a universal mode of regulation of RPTPs. While the D1 domain of RPTP μ was found to exist as a dimer, the amino-terminal helix–turn–helix of one D1 domain was not inserted into the active site of the other D1 domain. This resulted in an active site that was open and unhindered toward substrate binding. Hoffmann and co-workers concluded that homodimerization is not a common method of regulation. Several recent reports have suggested that heterodimerization may be a more generally applied method of regulation. Wallace et al. showed that the noncatalytic D2 domain of RPTP δ strongly binds to and inhibits the catalytic activity of the D1 domain from RPTP σ .¹⁴⁹ Weaker interactions between the D2 domain of RPTP δ as well as other RPTPs may play a role in regulating the catalytic activity of the D1 domains. Blanchetot and den Hertog demonstrated that RPTP α interacts with the D2 domain of a number of RPTPs including RPTP σ , RPTP α , LAR, RPTP δ , and RPTP μ .¹⁵⁰ These interactions were shown to involve the wedge structure of RPTP α -D1.

Although interactions between the D1/D2 domains of many RPTPs may indeed help in regulating their phosphatase activity, the discovery of pleiotrophin (PTN) as an in vitro and in vivo regulatory ligand of RPTP β (also referred to as RPTP ζ)¹⁵¹ has further complicated the picture on how RPTPs are regulated. PTN is an 18-kDa heparin-binding cytokine that signals a variety of different phenotypes in cells undergoing normal and deregulated cellular growth and differentiation. Meng et al.¹⁵² demonstrated that PTN is a natural ligand of RPTP β and upon binding to RPTP β reduces the catalytic phosphatase activity of RPTP β , resulting in increased levels of tyrosine-phosphorylated β -catenin. The mechanism by which PTN reduces the phosphatase activity of RPTP β for phosphorylated substrates has yet to be determined. Additional biochemical studies should further clarify the mechanism by which regulation of the phosphatase activity of RPTPs occurs and whether homodimerization or heterodimerization is a generalized mode of regulation.

Reversible intramolecular interactions between various domains contained within protein tyrosine phosphatases have been suggested to play a regulatory role. Recent work by Feiken et al. showed that intramolecular interactions may also be a method of regulation.¹⁵³ Using RPTP μ , the D1 catalytic domain was found to bind to an N-terminal region in the intracellular portion of RPTP μ . This noncatalytic region is termed the juxtamembrane (JM) region (aa 803–955) and is upstream from the D1 and D2 domains. The JM polypeptide could bind to both the D1 and D2 domains but could not bind to full-length RPTP μ , suggesting that the interactions between JM

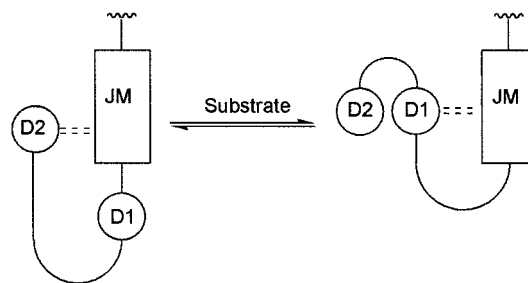


Figure 14. Proposed interactions between the JM domain and the D1/D2 domains in RPTP μ by Feiken and co-workers.¹⁵³

and D1 or D2 were strictly intramolecular. Removal of a large portion of the JM domain resulted in a loss in the catalytic activity of the D1 domain, similar to that observed with RPTP α and LAR,^{98,154} indicating that the JM/D1 interactions are essential for activity. The authors proposed (Figure 14) that in the inactive state the D2 domain of RPTP α interacts with JM. In the presence of substrate, the enzyme adopts a new conformation, forming interactions between JM and D1, stimulating the dephosphorylation of the substrate.

The SH2-containing PTPs provide the best examples of intramolecular interactions regulating enzyme activity. To date, only three SH2-containing PTPs (SHP-1, SHP-2, and corkscrew [*csw*], a *Drosophila melanogaster* homolog) have been identified.¹⁰ All three of these enzymes contain two SH2 domains followed by the catalytic domain and a C-terminal extension. While the enzymatic activity of SHPs are relatively low in comparison to other PTPs,¹⁵⁵ a 10-fold increase in k_{cat} is observed upon binding of a single phosphotyrosine peptide to one SH2 domain.^{156,157} Binding of biologically relevant diphosphorylated peptides at significantly lower concentrations in comparison to monophosphorylated peptides result in 100-fold increase in catalysis.¹⁵⁷ To understand how phosphatase activity is regulated by interaction of the SH2 domains with phosphoproteins, a mechanism was proposed based upon the structural determination of SHP-2.¹⁹ The crystal structure of SHP-2 (Figure 15) indicated that the N-terminal SH2 domain (N-SH2) was bound to the phosphatase domain, therefore blocking access to the active site (Figure 15). The carboxyl-terminal SH2 domain (C-SH2) makes minimal contact to either the N-terminal SH2 domain or the phosphatase domain. The phosphotyrosine-binding sites for both SH2 domains are located on the outside surface, easily accessible to solvent.

An explanation for the low catalytic activity of SHP-2 in the absence of ligand has been proposed based upon the interactions that are observed between the active site of the phosphatase domain and the N-terminal SH2 domain. The N-SH2 domain makes extensive surface contacts with the phosphatase domain over an area of 1208 Å², essentially preventing the binding of phosphorylated substrates. Critical interactions between the 4'-5 loop (Figure 15) connecting $\beta 4'$ and $\beta 5$ strands in the N-terminal SH2 domain are observed with the loop extending deep into the active site. These interactions include hy-

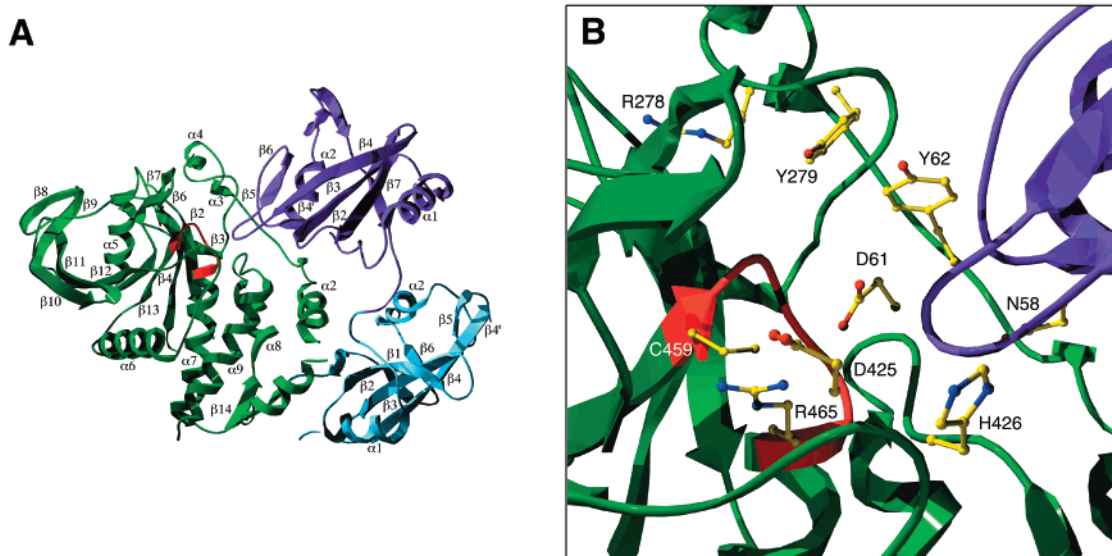


Figure 15. Ribbon diagrams of (A) SHP-2 and (B) an expanded view showing autoinhibition. The phosphate-binding loop is highlighted in red. The nomenclature used for the separate domains was that published by Hof and co-workers.¹⁹ The loop joining B4 and B5 of the N-terminal SH2 domain (purple) is inserted into the active site of the PTP catalytic domain (green), while the C-terminal SH2 domain (light blue) makes minimal contact to the remainder of the protein. Residues important for catalysis or interactions between domains are presented in Figure 6B. The diagram was generated from the crystal structure of SHP-2 published by Hof et al.¹⁹ using Swiss Pdb Viewer v3.5²³ and POV-Ray v3.1.

drogen bonding of Asp-61 of the N-SH2 domain with the active-site cysteine residue (Cys-459), which locks the SH2 domain into position. The insertion of the 4'-5 loop into the active site does not induce a conformational change in the general-acid loop as is observed with other PTPs.^{21,81} Instead, the active site remains in the opened, inactive form and closure of the general-acid loop would not be permitted.

The N-terminal SH2 domain of SHP-2 has been proposed by Hof et al. to act as an allosteric switch for phosphatase regulation. A comparison of the SHP-2 crystal structure¹⁹ to that of the N-SH2 domain without and complexed with phosphopeptides^{158,159} reveals conformational differences between the various forms of the N-SH2 domain. Upon binding of a phosphopeptide to the N-SH2 domain, conformational changes disrupt the interactions between the N-SH2 and phosphatase domains, eliminating the inhibitory effects of the N-SH2 domain.

2. Oxidative Regulation of the Active-Site Cysteine

Biological oxidants play an important role in many biological processes, including the regulation of growth factor function and tyrosine phosphorylation-dependent signal transduction.¹⁶⁰⁻¹⁶² It has been proposed that some of these effects are due to the inhibition of intracellular PTPs by biological oxidants.^{163,164} While there is substantial evidence for the biological oxidation of PTPs *in vitro*, more evidence is needed to confirm that PTPs are oxidatively regulated *in vivo*. It has been demonstrated that upon ligation of cell-surface receptors, including cytokine and growth factor receptors, a transient increase in the intracellular concentrations of hydrogen peroxide (H_2O_2) is induced within mammalian cells.¹⁶⁵⁻¹⁶⁷ PTP activity in crude cell extracts was shown to be inhibited in the presence of many oxidants, including H_2O_2 , and activity was restored upon the addition of thiol-

containing compounds such as dithiothreitol (DTT) and reduced glutathione (GSH).^{168,169} Epidermal growth factor (EGF) induced formation of H_2O_2 has been shown to affect the activity of PTP1B in A431 epidermoid carcinoma cells.¹⁷⁰ The site of oxidation of PTP1B was determined to be at the nucleophilic cysteine residue (Cys-121), and oxidative inactivation of PTP-1B is completely reversible.

Direct support that PTPs may be regulated through a redox mechanism and that the transient formation of H_2O_2 can target PTPs was obtained using the phosphatases LAR, PTP1, and VHR.¹⁶⁴ These phosphatases were found to be sensitive to inhibition by H_2O_2 , and activity could be restored by the addition of thiol-containing reagents. The nucleophilic cysteine was verified as the target of H_2O_2 inactivation in VHR and proposed to be the site of inactivation in LAR and PTP1. Results verifying the formation of a sulfenic acid intermediate were substantiated through the reaction of H_2O_2 -inactivated phosphatase with 7-chloro-4-nitrobenzo-2-oxa-1,3-diazole chloride (NBD-Cl, **1**) (Figure 16). NBD-Cl has been used previously to detect and identify cysteine sulfenic acid residues at the active sites of mutants of alkyl hydroperoxide reductase (AhpC) and native NADH peroxidase.¹⁷¹ Both AhpC and NADH peroxidase use a cysteine thiolate to reduce peroxide substrates with the concomitant formation of a cysteine sulfenic acid intermediate. NBD-Cl was used to react with both the cysteine thiolate and the cysteine sulfenic acid to produce two distinct intermediates with different absorbance spectra (Figure 16). The Cys-S-NBD adduct (**2**) shows a maximal absorbance at 420 nm, while the Cys-S(O)-NBD (**3**) adduct shows a maximal absorbance at 347 nm. Using native and H_2O_2 -oxidized VHR to represent all three of the phosphatases in the study, Denu and Tanner obtained conclusive evidence that a sulfenic acid intermediate

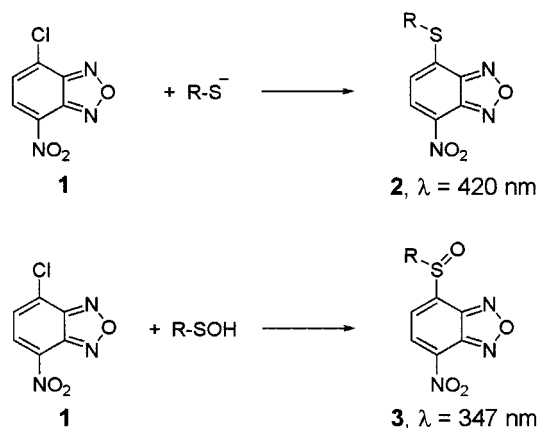


Figure 16. Expected products from the reaction of NBD-Cl (**1**) with cysteine thiolates or sulfenic acids.

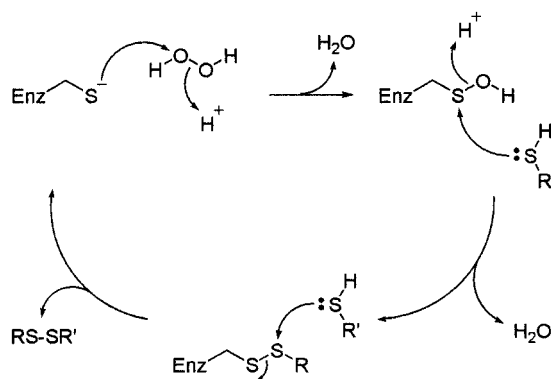


Figure 17. Proposed mechanism for the inactivation of PTPs and DS-PTPs via hydrogen peroxide oxidation and reactivation by sulfhydryl-containing compounds.¹⁷²

is formed upon oxidation of the nucleophilic cysteine residue by H₂O₂. Because the cysteine-sulfenic acid residue can be reduced back to the thiolate by a variety of biological reductants, the redox state within the cell may play a major role in the regulation of tyrosine phosphatase activity.

The cysteine sulfenic acid intermediate formed by reaction of the cysteine thiolate and hydrogen peroxide is a very reactive intermediate. The existence of this intermediate is only transitory and can be further oxidized to either a sulfinic or sulfonic acid form, both of which are irreversible processes and result in stable products. Using PTP1B, Barrett and co-workers generated a mixed disulfide with the active-site cysteine using either diamide and reduced glutathione or with glutathione disulfide (GSSG), which were characterized by mass spectral analysis.¹⁷² Enzyme activity could be regained upon addition of DTT, presumably by reducing the mixed disulfide. Activity could also be regenerated when the inactivated PTP1B (as the mixed disulfide) is incubated in the presence of the glutathione-specific dethiolase enzyme glutaredoxin, indicating that the inactivated form of PTP-1B is a glutathionyl mixed disulfide. Because of the instability of the sulfenic acid intermediate upon reaction of the cysteine thiolate with H₂O₂, it has been proposed that the final oxidized product leading to inactivation of the phosphatase is as a mixed disulfide (Figure 17).^{164,172} The physiological importance to PTP regulation remains to be fully explored, but the ability of the PTPs to be

regulated through oxidation of the catalytic cysteine residue in conjunction with other regulatory mechanisms is appealing and may explain how specific PTPs are positively or negatively regulated in the cell.

3. Regulation by Phosphorylation

The regulation of cellular processes is quite complex and can involve a number of mechanisms. One of the most common mechanisms, however, is through phosphorylation/dephosphorylation. A majority of the protein tyrosine phosphatases that have been discussed in this review act upon regulatory enzymes that govern important cellular events. Dephosphorylation of ERK2 by MKP-3, for example, results in loss of kinase activity and termination of cell-signaling events. Ironically, some of the PTPs themselves are phosphorylated. Several reports have identified phosphorylation of the PTP CD45 in T cells as an event that may regulate its activity.^{173–175} The effects of phosphorylation vary from phosphatase to phosphatase, however. One of the best examples of varied effects of phosphorylation upon phosphatases activity is observed with the dual-specificity phosphatases Cdc25A, Cdc25B, and Cdc25C. These dual-specificity PTPs participate in the tightly controlled regulation of the cell cycle. Hoffmann et al. demonstrated that phosphorylation of Cdc25A in the S phase of the cell cycle is dependent upon Cdc2/Cyclin E kinase activity and results in a 2–3-fold rate enhancement.⁵⁴ Cdc25C has also been shown to undergo phosphorylation. Phosphorylation of Cdc25C is required for the dephosphorylation and subsequent activation of Cdc2-cyclin B and entry of cells into M phase.⁵² Phosphorylation of Cdc25C by Cdc2-cyclin B resulted in a 4–5-fold increase in phosphatase activity but was not identified as an in-vivo substrate of the cyclin A-associated kinases. A human proliferation-related kinase (Prk) has recently been shown to not only interact with but also phosphorylate Cdc25C.¹⁷⁶ Prk has been demonstrated to regulate M phase functions.¹⁷⁷ Interestingly, Cdc25B also becomes phosphorylated but does not lead to an increase in activity nor does it participate in feedback loops with Cdc2-Cyclin complexes as observed with Cdc25A and Cdc25C. Baldin et al. presented data suggesting that Cdc25B is targeted for in vitro and in vivo degradation by the proteasome upon phosphorylation.¹⁷⁸ Phosphorylation of Cdc25B was dependent upon Cdc2-Cyclin A activity but not Cdc2-Cyclin B, suggesting another regulatory point in the cell cycle. Splice variants of Cdc25B (Cdc25B1 and Cdc25B2) have shown an increase in activity toward Cdc2-Cyclin B but can also dephosphorylate Cdc2-Cyclin A when Cdc2-Cyclin A is inactivated by phosphorylation.¹⁷⁹ Work by Nishijima et al. has also shown activation of Cdc2-Cyclin B by Cdc25B and suggests that Cdc25B activation of Cdc2-Cyclin B is the initial regulatory step that initiates mitosis through the activation of Cdc25C.¹⁸⁰ Combined, these results illustrate the delicate regulation that exists between both the Cdc25 phosphatases and Cdc2 kinases during the cell cycle. Brondello and co-workers recently observed an opposite effect whereby phosphorylation of MKP-1 by p42/p44^{MAPK} resulted in

stabilization of the phosphatase and increased half-life.¹⁸¹ It is unclear, however, whether phosphorylation leads to a truly more stable enzyme or protects from degradation of proteases that would normally degrade the unphosphorylated PTP.

The cytosolic phosphatase PTP-1B also undergoes phosphorylation. PTP-1B contains a total of three different phosphorylation sites that are dependent upon the activity of vastly different kinases. PTP-1B undergoes phosphorylation during the transition from G₂ to M in the cell cycle.¹⁸² A C-terminal region in PTP-1B contains three serine residues at positions 352, 378, and 386, all of which were phosphorylated. Protein kinase C (PKC) and Cdc2-Cyclin B were found to phosphorylate Ser-378 and Ser-386, respectively, but the kinase responsible for the phosphorylation at Ser-352 has not been identified. At the time, the effect of phosphorylation upon enzyme activity in PTP-1B was not determined and the physiological significance of phosphorylation was only speculated. It was later determined that phosphorylation at Ser-352 and Ser-386 not only occurs during mitosis, but also occurs as a result of osmotic shock and other environmental stresses.¹⁸³ It has been proposed that the same kinase activity responsible for phosphorylation during mitosis may also be active under cellular stress and may represent a novel protein kinase pathway.

A second phosphorylation site at Ser-50 has recently been identified.¹⁸⁴ The evolutionarily conserved dual-specificity kinases CLK1 and CLK2 were shown to phosphorylate PTP-1B at Ser-50, resulting in a 3–5-fold increase in phosphatase activity in vitro, while coexpression of CLK1 or CLK2 with PTP-1B in HEK 293 cells produced a 2-fold increase in activity. CLK1 and CLK2 also increase the catalytic activity of the related *S. cerevisiae* PTP-1B (YPTP1) by 2-fold. While the biological role of the CLK kinases has yet to be determined, it appears that PTP-1B may be an important cellular target for CLK phosphorylation.

It has been shown that PTP-1B dephosphorylates a number of proteins in response to insulin.¹⁸⁵ It was later determined that PTP-1B forms a complex with the insulin receptor in vivo and is phosphorylated at Tyr-66 and/or Tyr-152/153. The extent of phosphorylation and activation on PTP-1B was not determined, but mutagenesis of Tyr-66 and Tyr-152/153 substantially reduced the amount of phosphorylated PTP-1B as well as the extent of interactions between PTP-1B and the insulin receptor. PTP-1B was furthermore shown to be phosphorylated and interact with the epidermal growth factor receptor (EGFR).¹⁸⁶ Phosphorylation occurred specifically at Tyr-66 and resulted in a 3-fold increase in PTP activity. Additionally, two other PTPs undergo phosphorylation on tyrosine residues upon binding to physiologically relevant proteins. After platelet-derived growth factor (PDGF) stimulation, SHP-2 binds to and is phosphorylated by the PDGF receptor at Tyr-542.¹⁸⁷ The receptor-like PTP RPTP α is phosphorylated at position Tyr-789 and binds to the adapter protein GRB2, which may result in an attenuation in growth factor signaling by competing with receptor protein tyrosine

kinases for GRB2.¹⁸⁸ The existence of numerous phosphorylation sites within PTPs illustrates the complexity by which many of the phosphatases are regulated. Although the majority of PTPs do not appear to be regulated by phosphorylation, enough support exists to suggest that phosphorylation may be a regulatory mechanism for some members of the PTP family.

III. Serine/Threonine Specific Protein Phosphatases

A. Background

This section of the review will concentrate strictly on the structural and mechanistic work that has been published on the PPs in recent years. Also to be addressed is regulation of specific members of the PP family. For more detailed accounts on the serine/threonine specific PPs, PP1, PP2A, and PP2B (calcineurin), please refer to the corresponding authors whom have also contributed articles to this issue of *Chemical Reviews*.

The serine/threonine-specific phosphatases (PPs) constitute the second major class of protein phosphatases that catalyze the dephosphorylation of proteins containing phosphorylated amino acid residues. The PP class is divided into two distinct gene families, designated PPP and PPM. The PP's are partially categorized into families based upon regulatory and targeting domains that are associated with the catalytic domain, their sensitivity to a variety of different inhibitors, distinct metal requirements, and genetic homology.^{4,13,189–191} The PPP gene family consists of such subfamilies as PP1, PP2A, PP2B (calcineurin), and PP5 with a given family being further subdivided.¹⁹² PP1 is an important regulator of glycogen metabolism,^{193,194} and based upon observations on inhibition of PP1, as well as PP2A, by the tumor promoter okadaic acid, it may also act as a tumor suppressor.¹⁹⁵ PP2A has been proposed to participate in many regulatory roles including general metabolism, the cell cycle, and cellular signaling.^{196,197} PP2B is one of the most highly studied members of the PPP family and plays an important role in many signal transduction pathways. The most prominent role of PP2B is in T-cell receptor-mediated signal transduction in T lymphocytes.^{198,199} PP2B is activated upon binding of calmodulin and calcium^{200–203} and is a target of the immunosuppressive drugs cyclosporin A and FK506.^{204,205} Lambda protein phosphatase (λ -PP), a PPP isolated from bacteriophage lambda, exhibits many of the same characteristics as the other members of the PPP family but is of much smaller mass and has made an excellent model for study of the PPP gene family. The biological role of λ -PP remains to be determined.

The second gene family, PPM, consists of a large and varied family of phosphatases that are present in both prokaryotes and eukaryotes.²⁰⁶ PP2C is the defining member for this gene family. The PP2C subfamily shows a strong dependence for Mg²⁺ or Mn²⁺²⁰⁷ and exhibits no significant sequence homology with the PPP family members.^{13,190} Mammalian PP2C isolated from a number of sources, including

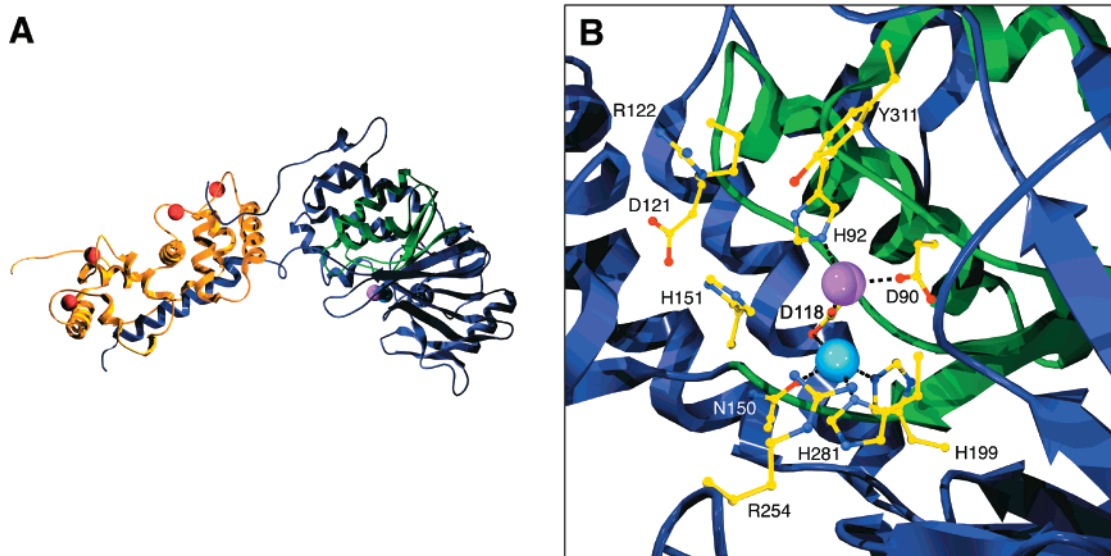


Figure 18. Ribbon diagram of (A) PP2B and (B) an expanded view of the active site showing the interaction of ligand residues and other amino acids important in catalysis. The β -subunit is in gold with the calcium atoms in red. The catalytic subunit is in dark blue with the β - α - β - α - β motif in green. The iron (pink) and zinc (light blue) are represented as spheres in both diagrams. Binding interactions between the metal centers and ligand residues are represented as black dotted lines. Water molecules were removed for clarity. The diagram was generated from the crystal structure of PP2B published by Kissinger et al.²²² using Swiss Pdb Viewer v3.5²³ and POV-Ray v3.1.

human, exhibits greater than 90% sequence homology between species, such as rabbit and rat. Mammalian PP2C exists in two major isoforms, PP2C α and PP2C β , which show 75% identity with each other. Three different isoforms of PP2C α (α -1, α -2, and α -3) have been isolated from HL60 monocytes.²⁰⁸ Within the PP2C β class, five separate isoforms (β -1, β -2, β -3, β -4, and β -5), which are splicing variants of the same mRNA, have been isolated from mice.^{209–211} PP2C appears to have a conserved role in negatively regulating MAPK (mitogen-activated protein kinase) pathways in several systems. PP2C has been shown to regulate the pheromone and osmoregulation pathways in yeast by acting on various MAP kinases and upstream regulators.^{212,213} PP2C is also hypothesized to regulate the stress-activated signal transduction pathway in fission yeast.²¹⁴ In plants, MP2C (a PP2C homolog) appears to down regulate the stress-induced MAPK pathway that is activated by drought, cold, wounding, and physical contact. In mammals, PP2C has been shown to down regulate the stress-activated p38 and JNK MAPK pathways.^{215,216}

B. The PPP Gene Family

1. Structure of the PPP Gene Family

The PPPs typically consist of a catalytic subunit/domain in association with regulatory or targeting subunits/domains that are important in defining the biological roles of these phosphatases. There is very little homology between these subunits and/or domains, with the exception of the catalytic domain. For example, PP2B contains the catalytic subunit A as well as well as a calcium-binding subunit B and calmodulin.^{6,13} The catalytic subunit of PP1 can be associated with at least 15 different regulatory subunits, including Gm, inhibitor-1, inhibitor-2, and p53BP2.¹³ The PPP family of phosphatases is further distinguished from the PPM family based upon

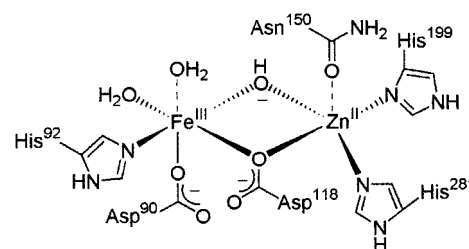


Figure 19. Schematic representation of the ligand environment in PP2B based upon the X-ray crystal structure reported by Kissinger et al.²²²

amino acid sequence. The catalytic domain contains a highly conserved active-site motif with the consensus sequence **DXH(X)**_{23–26}**GDXDXDR(X)**_{20–26}**GNH(E/D)** as is observed in PP1, PP2A, PP2B, and λ -PP.^{12,217} Interestingly, this general motif is also found in other phosphoesterases such as 5'-nucleotidases, RNA debranching enzyme, and 2'3'-cyclic nucleotide phosphodiesterases,²¹⁸ illustrating nature's conservation of this general method of phosphoesterase activity.

A common architecture consisting of a β - α - β - α - β scaffold was identified from the solution of X-ray structures of PP1^{219,220} and PP2B (Figure 18).^{221,222} This structural scaffold contains a dinuclear metal ion center which constitutes the active site. The identity of the metal ions in PP2B was determined to be Fe³⁺ and Zn²⁺ based upon electron paramagnetic resonance (EPR) studies and the presence of stoichiometric amounts of iron and zinc in the enzyme.²²³ The identity of the metal ions in PP1 has not been identified, but the enzyme shows the same structural motif and coordination environment as that observed with PP2B. Regardless of the metal ions in the active site, metal ion 1 (M1, Fe³⁺ in PP2B) is octahedrally coordinated by two aspartate residues (D90 and D118 using PP2B numbering, Figure 19), a histidine residue (H92) and three water molecules

(W1, W2, and W3). The second metal ion (M2, Zn^{2+} in PP2B) is in a distorted trigonal bipyramidal coordination environment with an aspartate, asparagine, and two histidine residues (D118, N150, H199, and H281 in PP2B) as well as a bridging water molecule, W1. This coordination environment is identical to that of purple acid phosphatases (PAP) with the exception that a tyrosine residue is substituted for a water ligand on the iron atom (M1) of PP2B.^{224–226} This ligand substitution in PAPs results in a tyrosine-to-iron charge-transfer band at approximately 560 nm which gives the enzyme a purple color.²²⁷

2. Catalytic Mechanism of the PPP Family

Toward elucidating the catalytic mechanism employed by the PPs, most work has been performed with PAP, PP2B, and λ -PP. In addressing the catalytic mechanism of PP2B, Graves et al. presented three initial mechanisms.²²⁸ The first involved directed nucleophilic assistance by a group on the enzyme to form an initial enzyme–phosphate intermediate. A second mechanism proposed direct displacement of the phosphate in the substrate by a water molecule that is coordinated to the metal centers. The third hypothesis involved a unimolecular breakdown of the metal–substrate complex. While the formation of a phospho–enzyme intermediate has been observed in other phosphatases,^{229–231} including the PTPs,^{24,100,104–106} results from steady-state kinetic experiments suggested that a phospho–enzyme intermediate was not formed in PP2B. Martin and associates were unable to demonstrate phosphotransferase activity, which also supported the lack of formation of a phospho–enzyme intermediate. At the time, however, the authors could not rule out the other two mechanisms. Product inhibition studies later indicated that both phosphate and *p*-nitrophenol act as competitive inhibitors to PP2B, providing evidence that PP2B utilizes a random uni-bimolecular mechanism.²³² These results suggested that an intermediate is not formed in the enzyme-catalyzed reaction because if a phospho–enzyme intermediate were formed the leaving group must first depart in an ordered fashion before hydrolysis of the phospho–enzyme intermediate can occur.²³³

Additional support for direct hydrolysis of the phosphate monoester by water was obtained using bovine spleen PAP and the chiral substrate *S*_P-2',3'-methoxymethylidene-ATP- γ -¹⁷O₂ γ -¹⁸O₃S (**4**).²³⁴ The for-

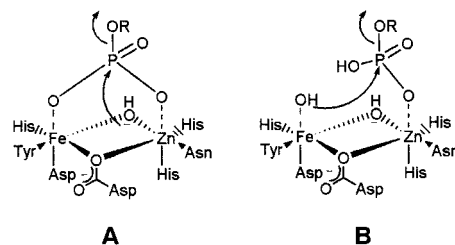
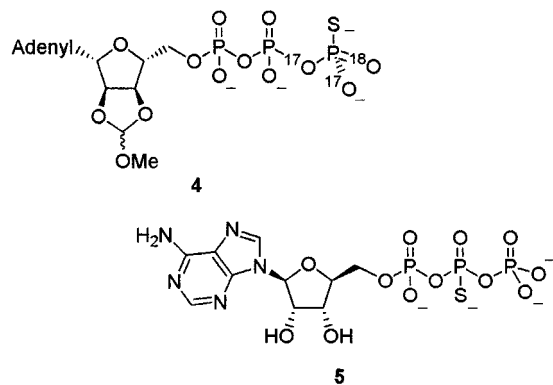


Figure 20. Possible mechanistic schemes for phosphate monoester hydrolysis by purple acid phosphatase proposed by Wang and co-workers.²³⁷

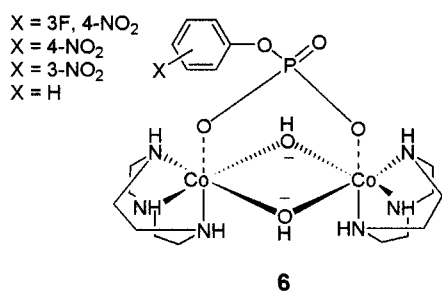
mation of *R*-[¹⁶O, ¹⁷O, ¹⁸O]thiophosphate by PAP was coupled to the enzymatic incorporation of thiophosphate into adenosine 5'-(2-thiotriphosphate) (**5**) and then analyzed by ³¹P NMR. Interpretation of the ³¹P NMR indicated an inversion of configuration in the formation of thiophosphate by PAP. If a phospho–enzyme intermediate were generated by PAP, a net retention of configuration at phosphorus would have occurred upon hydrolysis of the intermediate, resulting in a distinct ³¹P NMR spectrum. Through the use of solvent isotope effects and isotope exchange studies, Martin and Graves concluded that no phospho–enzyme intermediate is formed and that proton transfer from a coordinated water molecule may occur during binding of substrate.²³⁵ Collectively these studies provide compelling evidence for the lack of a phospho–enzyme intermediate during catalysis and supports the involvement of a nucleophilic source such as one of the water ligands instead of a nucleophilic side-chain residue.

The source of the nucleophile has been investigated through the use of enzyme analysis and model studies. Through a comparison of the coordination environment around the metal atoms in PAP and PP2B, two different water molecules may be the potential nucleophile for both enzymes, either the bridging water molecule (as a hydroxide ion) or the water ligand on iron.^{222,225} Crystal structures of PAP or PP2B with phosphate and tungstate^{219,220,225} show the formation of a bidentate bridge of the phosphate oxoanions to the metal centers (Figure 20, A). If this model represents the model of substrate binding of the active site, the only nucleophile available for hydrolysis would be the hydroxide ion bridging the two metals. The alternative would be the extra water molecule, which is a ligand to only the iron atom (Figure 20, B). This water molecule would be activated enough to undergo nucleophilic displacement of the phosphate residue on the substrate. Using bovine spleen (BS) or porcine uterus (PU) PAP, both Pinkse²³⁶ and Wang²³⁷ characterized ternary enzyme–phosphate–fluoride complexes that may represent the enzyme–substrate complex just prior to hydrolysis. Both groups showed that fluoride is a noncompetitive inhibitor at pH 5.0, the pH optimum for these enzymes. Through the use of kinetics and EPR spectroscopy with BSPAP–F–PO₄²³⁶ or EPR analysis with the PUPAP–F–PO₄ complex,²³⁷ both groups proposed that the fluoride ion was a ligand to the trivalent iron metal atom, displacing the water ligand. Unexpectedly, when PUPAP–PO₄ was analyzed by Raman spectroscopy or EXAFS,²³⁷ the data



suggested that the fluoride ion displaced the hydroxide bridge. Because of these results, Wang et al. proposed a mechanism by which, upon binding of substrate, the bridged hydroxide ion is shifted toward the zinc metal (M^{2+}) (Figure 20, A). This distorted diamond center is thought to increase the nucleophilicity of the hydroxide ion in hydrolysis.

Model systems have also provided some insight into the possible catalytic mechanism employed by the PPPs. Chin and co-workers addressed the reactivity of diesters coordinated to simple dinuclear Co(III) complexes.^{238–240} Recently, Chin and associates reported on the reactivity of the dinuclear Co(III) complex $[Co_2(tacn)_2(OH)_2\{O_3P(OAr)\}]^{2+}$ (**6**) ($tacn = 1,4,7$ -triazacyclononane) coordinated to various phosphorylated substrates, which further supports the role of the bridged hydroxide ion acting as the nucleophile. From a pH–rate profile and ^{18}O -labeling



experiments, the hydroxide bridging the two cobalt atoms was found to directly participate in hydrolysis. When these results are combined with those of Wang and associates,²³⁷ strong evidence exists that the origin of the nucleophile used by the PPP family of phosphatases is the bridging water molecule.

Before the crystal structures of many of the PPP family members were solved, 11 highly conserved residues were identified based upon the sequence alignment of many different PPs.^{12,217} The role of many of these residues in catalysis and substrate binding were initially examined with λ -PPP.²¹⁷ Mutations in Asp-20, His-22, Asp-49, His-76, and Glu-77 showed no significant changes in K_m , using $pNPP$ as substrate, suggesting that these residues play no direct role in substrate binding. Increases in the K_m for Mn^{2+} with mutations at Asp-20, His-22, Asp-49, and His-76 were observed and suggested a role for these residues in metal binding and/or catalysis. When residues Arg-53 and Arg-72 were mutated to alanines, a slight but noticeable increase in K_m for both mutants was observed when $pNPP$ was used as the substrate, indicating that both residues may be important for substrate binding and, therefore, may also be important in alignment of the substrate for hydrolysis. Arginine residues have been frequently identified as phosphate-binding residues.⁹⁴

After the publication of the crystal structures of PP1²¹⁹ and PP2B,^{221,222} many of the conserved residues were found to be actual ligands to the metal atoms. These residues were identified as Asp-90, His-92, Asp-118, Asn-150, His-199, and His-281 (using PP2B numbering, Figures 18 and 19). Using PP1, Zhang et al. showed that mutation of Asn-124, His-66, His-248, Asp-64, and Asp-92 resulted in a sig-

nificant loss in enzyme activity.^{241,242} These observations supported the role of these residues in metal binding as suggested by the crystal structure of PP1.²¹⁹ The importance of the ligand residues in PP2B was further illustrated by Mondragon et al. using alanine-scanning mutagenesis.²⁴³ Using this method, mutation of the metal-binding residues to alanine resulted in loss of phosphatase activity, supporting and expanding the work published by Zhuo and co-workers.²¹⁷ Also, mutation of residues His-151, Arg-122, and Arg-254 to alanine resulted in a dramatic decrease in activity, further supporting Zhuo's initial observations using λ -PP.

Mutation of His-76 in λ -PP to asparagine and the equivalent residue in PP2B (His-151) to glutamine also resulted in enzymes with decreased catalytic activity.²⁴⁴ Interestingly, these mutants showed changes in their corresponding EPR spectra when compared to the native enzymes. These changes indicated that disruption of the ligand environment around the iron center had occurred, possibly as a result of the removal of a hydrogen bond that may be present between the histidine residue and a ligand-bound water molecule.

Three groups have investigated the role of the conserved arginine residues in PPP catalysis. It has been demonstrated that a decrease in activity is observed in λ -PP, PP1, and PP2B when the conserved arginine residues are mutated.^{217,241–243} In the crystal structures of PP1^{219,220} and PP2B,^{221,222} these invariant arginine residues were shown forming hydrogen bonds with the oxoanions of either phosphate or tungstate, stabilizing their position in the active site. It is possible that these residues may be important in not only binding of substrate, but also aligning the substrate over the bridging hydroxide ion for hydrolysis.

As mentioned previously with respect to the elucidation of the catalytic mechanism employed by PTPs, (V/K) heavy-atom kinetic isotope effects have provided tremendous insight into the transition state of these enzymes. This method has also been employed successfully to examine the transition state in PP-catalyzed reactions. Using $pNPP$ as substrate for PP2B, the extent of bond formation and cleavage as well as charge development in the transition state were examined at the pH optimum of 7.0 and also at 8.5.²⁴⁵ As presented in Table 3, an increase in $^{18}(V/K)_{bridge}$ and $^{15}(V/K)$ was observed as the pH of the assay increased. At pH 8.5, the value of $^{18}(V/K)_{nonbridge}$ was similar to that observed for non-catalytic hydrolysis. Together, these results suggested that P–O bond cleavage is partially rate-limiting at the pH optimum but can be increased at higher pH. Analysis of λ -PP produced kinetic isotope effects²⁴⁶ (Table 3) which were very similar to those observed for the PTPs (Table 1). Because of the magnitude of the kinetic values, P–O bond cleavage is fully rate-determining for λ -PP, unlike that observed for PP2B. On the basis of the similarity of the values, the PPs appear to utilize a dissociative transition state similar to the PTPs.

In the same study in which the transition state of native PP2B was examined, Hoff et al. investigated

Table 3. Isotope Effects for Native and Mutant Enzymes of PP2B and λ -PP

enzyme	enzymatic reactions		
	$^{15}(V/K)$	$^{18}(V/K)_{\text{bridge}}$	$^{18}(V/K)_{\text{nonbridge}}$
PP2B, pH 7 ^b	1.0006 ± 0.0005	1.0072 ± 0.0011	
PP2B, pH 8.5 ^b	1.0014 ± 0.0001	1.0115 ± 0.0112	0.9942 ± 0.0007
PP2B, pH 8.5, 5mM Mn, pH 7 ^b	1.0011 ± 0.0003	1.0103 ± 0.0014	
λ -PP, pH 7.8 ^c	1.0006 ± 0.0003	1.0133 ± 0.0006	0.9976 ± 0.0003
λ -PP-H76N, pH 7.8 ^c	1.0016 ± 0.0003	1.0183 ± 0.0009	0.9976 ± 0.0001
	solution reactions ^a		
	^{15}k	$^{18}k_{\text{bridge}}$	$^{18}k_{\text{nonbridge}}$
monoanion in water	1.0005 ± 0.0002	1.0106 ± 0.0003	1.0224 ± 0.0005
dianion in water	1.0034 ± 0.0002	1.0230 ± 0.0005	0.9993 ± 0.0007
dianion in <i>tert</i> -butyl alcohol	1.0039 ± 0.0003	1.0202 ± 0.0008	0.9997 ± 0.0016

^a From Hengge, A. C.; Edens, W. A.; Elsing, H. *J. Am. Chem. Soc.* **1994**, *116*, 5045–5049. ^b From Hengge, A. C.; Martin, B. L. *J. Am. Chem. Soc.* **1997**, *36*, 110185–10191. ^c From Hoff, R. H.; Mertz, P.; Rusnak, F.; Hengge, A. C. *J. Am. Chem. Soc.* **1999**, *121*, 6382–6390.

the role of His-76 in catalysis.²⁴⁶ When this residue was mutated to asparagine, the mutant showed V/K values approximately 350-fold less than the native enzyme. The V/K pH–rate profile for the H76N mutant was very similar to the bell-shaped curve observed with the native enzyme, however, the pH-dependency of the H76N V/K values at higher pH ranges were slightly less than that observed for the wild-type enzyme. The results from the pH profile studies suggested that His-76 might not be the protonated residue (general acid) having a pK_a value of approximately 7. The $^{15}(V/K)$ kinetic isotope effect for the His76Asn mutant (Table 3) was slightly higher than the wild-type enzyme, indicating that there was slightly less charge neutralization of the leaving group in the transition state compared with native enzyme. If the leaving group was departing with a full negative charge, a much larger $^{15}(V/K)$ effect would have been observed. While these results do not substantiate the role of this conserved histidine residue in acid/base catalysis, it is ideally positioned to donate a proton to the leaving group.

On the basis of the available crystal structures, mutagenesis experiments, and (V/K) kinetic isotope studies, the following mechanism is proposed (Figure 21). This mechanism is similar to that reported by Rusnak and Mertz⁶ inasmuch that His-151 (PP2B numbering) acts as a general acid/base during catalysis. In the active state (Figure 21, A), the ferric iron is ligated to an additional water molecule and the nonligated histidine is protonated. The substrate is aligned in the active site (Figure 21, B) by the arginine, and upon binding of the oxoanions of phosphates to the metal atoms, hydrolysis is initiated. Perturbation of the diamond center upon substrate binding shifts the bridging hydroxide anion closer to the zinc cation, increasing the nucleophilicity of the hydroxide anion for hydrolysis (Figure 21, B). As observed by the (V/K) kinetic isotope effects, substantial bond cleavage in the bridge oxygen atom develops, with minimal bond formation between the phosphorus atom and the incoming hydroxide nucleophile (Figure 21, C). As the leaving group departs, it is protonated by the histidine residue (His-155), which is acting as the general acid. This would generate the phosphate complex (Figure 21, D) which has been observed in many crystal structures.^{219,221,222}

Expulsion of inorganic phosphate and deprotonation of a ligated water molecule by His-151, acting as a general base, would then regenerate the active form of the enzyme (Figure 21, A).

C. The PPM Gene Family

1. Structure of the PPM Family

PP2C is the defining member of the PPM family of protein phosphatases. When PP2C was initially isolated in conjunction with PP2A from rat liver,^{247–250} it was placed alongside the other PPP family members. PP2C remained in the PPP family for several years even though PP2C exhibited an absolute requirement for Mg^{2+} or Mn^{2+} to maintain catalytic efficacy.^{247,248} Later, sequence alignment with PP1, PP2A, and PP2B showed no homology to that of PP2C, suggesting that PP2C was unrelated to the PPP family and as such represented a separate PP gene family.¹⁹¹

Mammalian PP2C was initially found to exist as two highly conserved isoforms (α and β) which show approximately 70% sequence homology;^{251–253} however, each isoform is highly conserved (>90%) between species such as humans, rats, and rabbits. A more recently discovered isoform (PP2C γ) has been reported but shows only 34% sequence identity to the α - and β -isoforms.²⁵⁴ Unlike PP2C α and PP2C β , PP2C γ contains an additional acidic domain consisting of 54 amino acids, 40 (75%) of which are either aspartate or glutamate residues. The function of this domain has yet to be determined but may be required for cellular targeting. Unlike the PPP family, mammalian PP2C has not been identified in tight association with any other subunits.

Sequence alignment of the eukaryotic PP2C family has identified 11 motifs that have also been observed in sequences obtained from fungal and bacterial origin.²⁰⁶ These motifs are distributed along the entire length of the amino acid sequence. Eight of these structural motifs contain a total of 14 highly conserved amino acid residues that may be required for substrate binding, specificity, or catalysis. The crystal structure of PP2C α has been solved and has shed some light on the potential role of some of these conserved residues.²⁵⁵ The crystal structure of PP2C

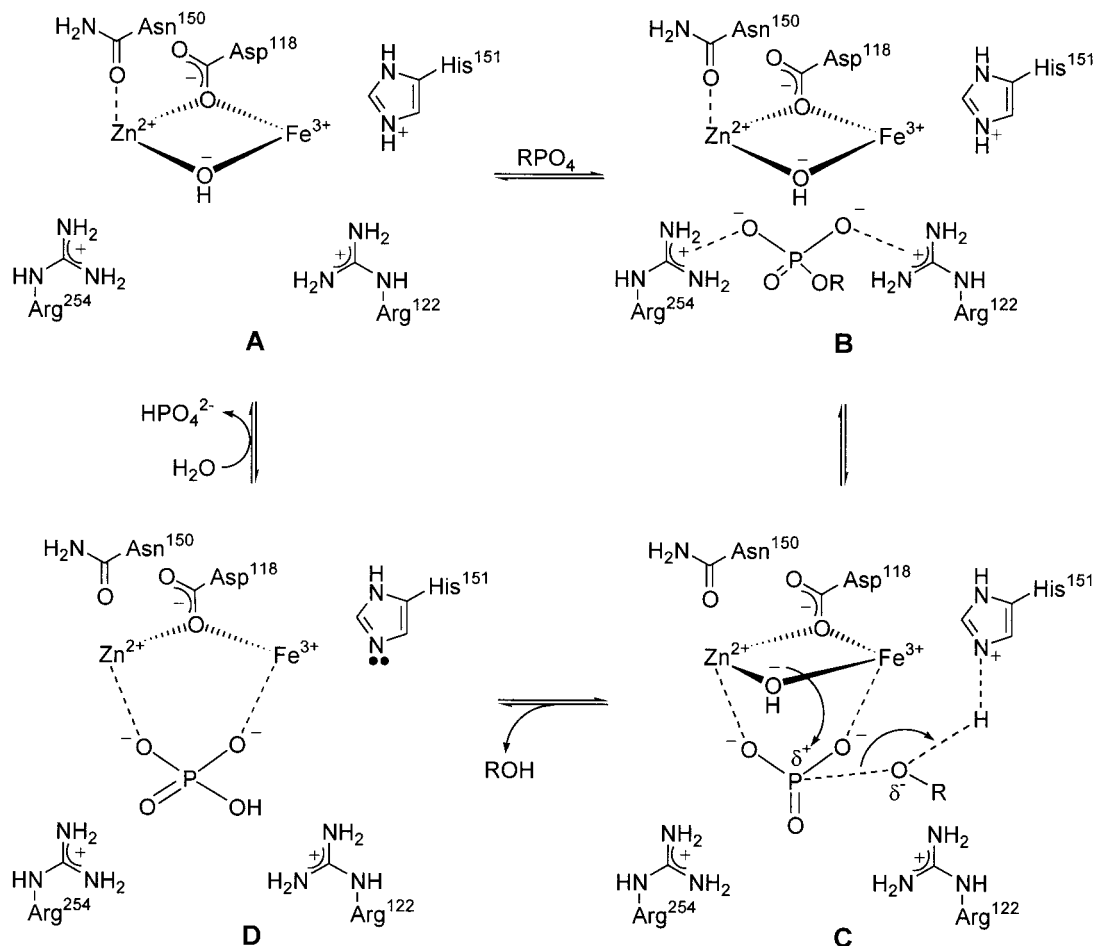


Figure 21. Proposed mechanism utilized by the PPP gene family with designated amino acid residues believed to play a role in catalysis. The mechanism is similar to that published by Rusnak and Mertz⁶ inasmuch that His-151 is acting as a general acid/base. Amino acid numbering is for PP2B (calcineurin).

was obtained with two Mn²⁺ ions bound in the active site (Figure 22). These ions are positioned at the end of a β -sandwich that is surrounded by α -helices. The manganese ions are hexacoordinated and approximately 4 Å apart. Both metals share a water molecule and an aspartate (Asp-60) to make a complex (Figure 22) that resembles that observed for PP1^{219,220} and PP2B^{221,222} (see Figures 22 and 23). Three water molecules and two additional aspartate residues, Asp-239 and Asp-282, coordinate the manganese ion that occupies site M1. The second metal center, M2, is coordinated to four water molecules, the backbone carbonyl of Gly-61, and the bridging aspartate residue (Asp-60). A phosphate molecule was also present in the crystal structure, which has provided some evidence that Arg-33, which is also highly conserved in many eukaryotic PP2C family members, may play an important role in substrate binding or catalysis. Arg-33 appears to position the phosphate directly above the bridged water molecule in the active site. This observation has led Das and co-workers to propose that PP2C catalyzes dephosphorylation using a mechanism similar to that proposed for PP2B and other PPP enzymes.²⁵⁵ Besides the quaternary structure that surrounds the active site, a 90-residue C-terminal domain that consists of three α -helices is present, which further distinguishes mammalian PP2C enzymes from other sources such as those

found in yeast and bacteria. This C-terminal domain is far removed from the active site and therefore may be a site of regulation, substrate specificity, or targeting.

2. Catalytic Mechanism of the PPM Gene Family

With the publication of the crystal structure of the PP2C α bound with Mn²⁺,²⁵⁵ a similar mechanism to that of the PPP family was proposed. However, very little is actually known about the catalytic mechanism utilized by these phosphatases. Extensive kinetic analysis of PP2C α has been performed by Fjeld and Denu, who provided some information on PP2C α -catalyzed reactions.²⁵⁶ PP2C has long been characterized as a Mg²⁺- or Mn²⁺-dependent protein phosphatases.¹⁹¹ Other ions such as Ca²⁺, Ni²⁺, and Zn²⁺ have been shown to inhibit the enzyme, possibly by competing with Mn²⁺ or Mg²⁺ for the active site.²⁵⁷

Fjeld and Denu observed the effects of Mg²⁺, Mn²⁺, Ca²⁺, Ni²⁺, and Zn²⁺ as well as other divalent metal ions on PP2C catalysis.²⁵⁸ Surprisingly, Fe²⁺ was over 1000-fold better than Mg²⁺ with respect to the steady-state parameters k_{cat} and V/K .²⁵⁸ A pH-rate profile of PP2C α using Mn²⁺ and Mg²⁺ with *p*NPP as substrate identified two critical ionizations required for activity.²⁵⁸ One ionization with a pK_a value of 7 must be unprotonated, while an ionization with a pK_a value of 9 must be protonated for activity. It was

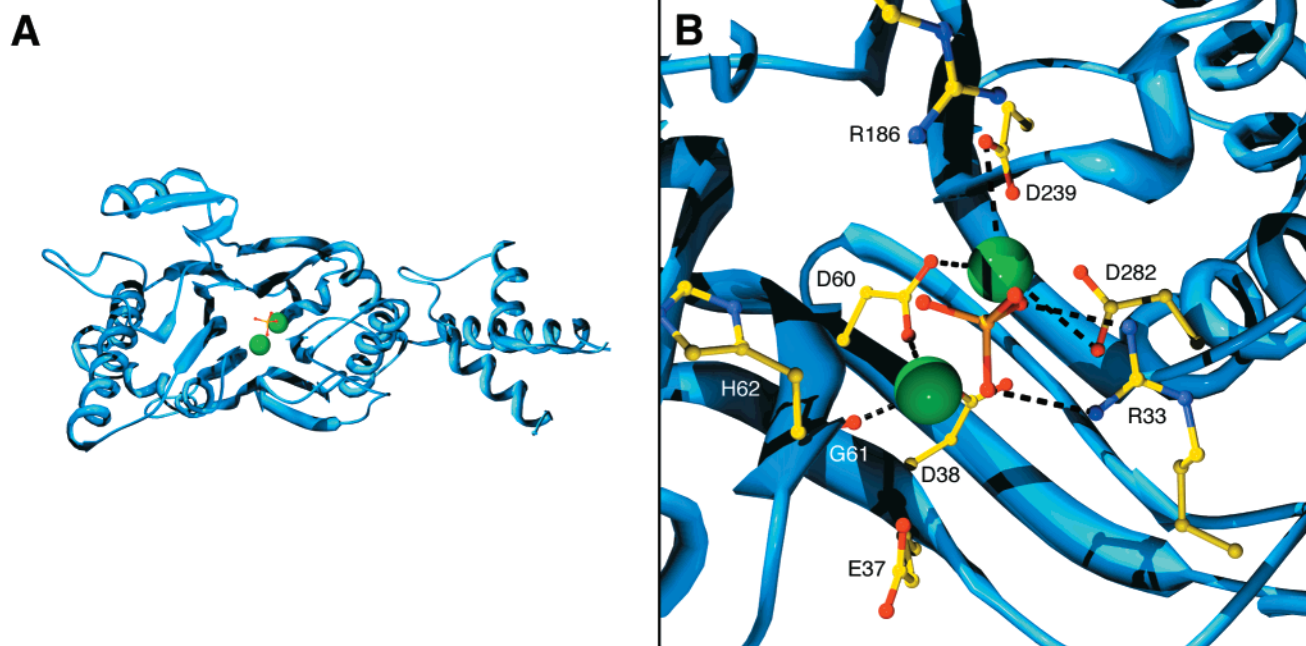


Figure 22. Ribbon diagram of (A) PP2C α and (B) an expanded view of the active site showing the two manganese atoms (represented as green spheres) with the ligand residues in yellow. Bonding interactions are represented as dashed lines. A phosphate residue (orange) is acting as a ligand to the two metal centers. Water molecules were removed for clarity. The diagram was generated from the crystal structure of PP2C α published by Das et al.²⁵⁵ using Swiss Pdb Viewer v3.5²³ and POV-Ray v3.1.

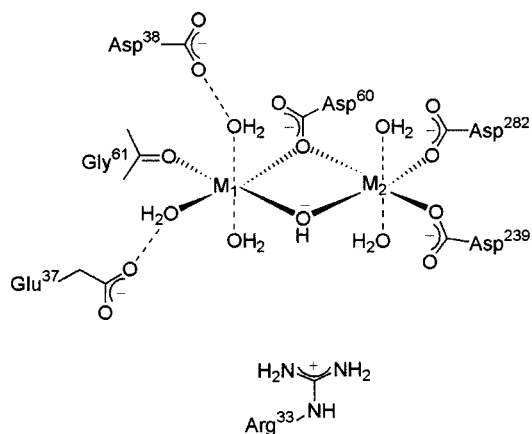


Figure 23. Schematic representation of the ligand environment in PP2C α based upon the X-ray crystal structure reported by Das et al.²⁵⁵ Arg-33 hydrogen bonds to the phosphate residue in the crystal structure.

proposed that the ionizable group having a pK_a value of approximately 7 might be the water molecule that bridges the two metal atoms in the active site. It has been proposed by some that the nucleophile in metallohydrolases is an activated water molecule with a $pK_a \sim 7$.^{259,260} The identity of the other ionizable group having a pK_a value of approximately 9 has not been determined with certainty. The authors wished to mention that the crystal structure of PP2C reported by Das et al.²⁵⁵ was obtained at pH 5. Fjeld and Denu demonstrated that the enzyme is improperly protonated at this pH.²⁵⁸ Interestingly, in the crystal structure of PP2C α , a conserved histidine residue (His-62) was located near the active site but the side chain was positioned too far away to act as a general acid/base and, instead, hydrogen bonds with an aspartate residue (Asp-199). It is difficult to

propose a role for many of the residues that reside close to the active site, because at this pH the environment surrounding the active site may not represent the active form of the enzyme. If the crystal structure of PP2C α can be obtained using a pH closer to the pH optimum so that all of the side chains are properly protonated, it can be determined whether the environment around the active site at the pH optimum is different than that reported by Das and co-workers and more accurately reflects the active state of the enzyme.²⁵⁵

Steady-state and inhibition studies indicated a sequential reaction pathway for PP2C α in which metal ions bind prior to binding substrate while phosphate is the last product to be released.²⁵⁸ Pre-steady-state studies revealed an initial "burst" of product formation at pH 8.5, which is consistent with the phosphate release being the rate-limiting step under these conditions. Also of note, PP2C α was shown to have a greater preference for diphosphorylated substrates, especially when the two phosphorylated sites are in close proximity to each other.

From these studies, several issues remain unresolved. Further studies need to address whether a phospho-enzyme intermediate is formed during catalysis by PP2C α . Fjeld and Denu, however, did not observe a phospho-enzyme intermediate during their studies.²⁵⁸ Also, the crystal structure of PP2C α ²⁵⁵ does not show a side-chain nucleophile around the active site, further suggesting that the nucleophile may be the bridged water molecule. This would imply that PP2C α hydrolyzes phosphate esters using a mechanism very similar to that proposed for the PPP gene family. The identity of the ionizable group having a pK_a value of approximately 9 has not been determined. Because the active-site metal atoms

make fewer contacts with the enzyme in comparison to PP1, PP2B, or PAP, the residue having a pK_a of ~ 9 may play an important role in maintaining the three-dimensional structure of the active site. As observed with λ -PP²¹⁷ and PP2B,²⁴³ mutating any of the residues that are ligands to the metal atom results in a dramatic decrease (up to 40 000-fold) in activity, due to altering the structure of the coordination environment around the metal atoms. The authors are currently examining the role of the 14 conserved residues in PP2C α through site-directed mutagenesis, which will provide further information on the specific role of each conserved residue. Of particular interest is residue His-62, which as previously mentioned could be repositioned toward the metal cations when the enzyme is in the correctly protonated state. Further biochemical studies will expand our current knowledge on the catalytic mechanism utilized by the PPM gene family.

D. Regulation of Serine/Threonine Phosphatases

This section of the review will only cover the possible regulation of PP2C in mammalian cells. For a detailed account of regulation in PP1, PP2A, and PP2B (calcineurin), please refer to the corresponding reviews in this issue of *Chemical Reviews*.

While little is known about the catalytic mechanism utilized by PP2C, even less is known about its regulation. Currently, there are two potential modes of regulation that have been proposed: regulation by phosphorylation and redox control. Phosphorylation of PP2C has been demonstrated by Tamura and associates, both in vitro and in vivo, using either *Saccharomyces cerevisiae*²⁶¹ or COS7 cells.²⁶² The sites of phosphorylation were identified as Ser-375 and/or Ser-377; however, physiological effects using the double mutant S375A/S377A were not determined. While phosphorylation may be a method of regulation of PP2C activity, additional research on the physiological role of phosphorylation is required before this hypothesis can be substantiated.

Redox regulation of PP2C may be a more effective and specific method to regulate its activity. It was initially proposed by Pato and Kerc that the identity of the metal ion used in catalysis by PP2C may play a role in its regulation.²⁵⁷ The important discovery by Fjeld and Denu, that PP2C α activity is greatly enhanced in the presence of Fe²⁺, strongly suggests that Fe²⁺ may be an in vivo metal in the active site.²⁵⁸ PP2C α was shown to have a strict requirement for at least one Fe²⁺ ion; however, the enzyme may also accommodate an Fe³⁺-Fe²⁺ center. While it has yet to be determined whether PP2C α can also accommodate an Fe³⁺ ion, the oxidation state of one or both metal ions could be a target of regulation. PAP is believed to contain a mixed valence diiron center which can also be represented as an Fe³⁺-Fe²⁺ metal center.²⁶³ PP2B is observed having an Fe³⁺-Zn²⁺ metal center²²³ but can be reconstituted to contain an Fe³⁺-Fe²⁺ center.²⁶⁴

If an iron center is truly the in vivo metal in the active site of PP2C, an interesting method of regulation can be proposed. In 1996, Klee and associates observed the in vitro and in vivo protection of PP2B

from oxidative damage by superoxide dismutase.²⁶⁵ This effect on PP2B activity has also been observed more recently by both in vitro²⁶⁶ and in vivo studies.²⁶⁷ Sommer and co-workers demonstrated that PP2B activity can be affected by a number of biological oxidants such as hydrogen peroxide and superoxide, while reductants such as glutathione and ascorbate protect from deactivation.²⁶⁶ The authors also observed inactivation of PP2C α in the presence of superoxide, which can be protected with superoxide dismutase, but not catalase (unpublished results). Superoxide is likely targeting either the iron center or modifying an amino acid residue close to the active site. It is possible that superoxide is oxidizing the lone Fe²⁺ in PP2B to Fe³⁺, thus affecting the requisite oxidation state of the dinuclear metal center. Alternate sites of oxidation, however, include active-site histidines that are either ligands to the metal center or are required in catalysis. There is precedence for the oxidation of critical histidine residues in enzymes that also contain a metal-binding site. Such examples include iron regulatory protein 2,²⁶⁸ Cu-Zn-superoxide dismutase,²⁶⁹ and alcohol dehydrogenase II.²⁷⁰ The oxidized residue is believed to be 2-oxo-histidine. It is thought that this oxidized derivative is the result of the initial reaction of iron with a highly reactive oxygen species (superoxide) to form a reactive intermediate, possibly a hydroxy radical. This initial intermediate may then oxidize a histidine that is in close proximity to the metal center. This hypothesis could also explain PP2B's susceptibility to superoxide, because PP2B not only has histidine residues that are coordinated to the iron center but also contains a histidine residue that may participate in acid/base catalysis. Our laboratory is currently addressing the issue of histidine oxidation as a potential site of oxidative regulation in PP2C catalysis. PP2C is involved in down-regulating the stress response in the cell; therefore, oxidative regulation of PP2C may be a way of ensuring that the stress response is not terminated. Redox regulation of the metal center or a side chain of a residue may be important in controlling catalysis. Further studies are currently underway to address these issues.

IV. Mechanistic Comparisons between Protein Phosphatases and Alkaline Phosphatases

While this review has focused exclusively on the mechanistic and structural aspects of protein phosphatases, the alkaline phosphatases (APs) share many mechanistic similarities between the PTP and PP gene families. Several excellent reviews on alkaline phosphatase structure and mechanism have been published over the years, and the authors would like to direct the reader to more recent reviews for a more detailed discussion on this topic. The brief summary that follows was derived from recent reviews by Holtz and Kantrowitz²⁷¹ as well as Coleman.²⁷²

Alkaline phosphatase is a nonspecific phosphoesterase found in a variety of organisms ranging from bacteria to yeast and mammals. *E. coli* AP is the prototype for all of the alkaline phosphatases, and a predominant amount of crystallographic, NMR, and

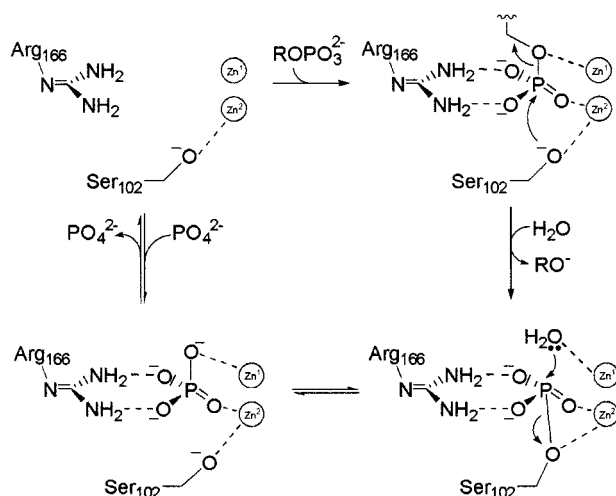


Figure 24. Proposed catalytic mechanism employed by the alkaline phosphatases. In the active state, the catalytic serine residue is coordinated to Zn2. Upon substrate binding, the oxyanions of the substrate form salt bridges to Arg-166 and Zn2, aligning the phosphate for nucleophilic attack by Ser-102. Upon removal of the leaving group from the active site, a water molecule that is activated by coordination to Zn1 hydrolyzes the phosphoserine intermediate to form the noncovalently bound phosphate-enzyme intermediate. Displacement of phosphate from the active site then regenerates the active enzyme.

kinetic studies have been performed with this enzyme. For maximal activity, AP requires a total of three divalent metal atoms in the active site (two zinc atoms and one magnesium at sites M1, M2, and M3, respectively). An aspartate residue (Asp-51) bridges the zinc and magnesium atoms (positions M2 and M3, respectively), similar to that observed for PP2B (Asp-118) and PP2C α (Asp-60). A serine residue (Ser-102) is located at the base of the active site and becomes phosphorylated upon removal of the leaving group. This serine residue is activated by coordination to zinc at position M2. Interestingly, the serine residue is not absolutely required for catalysis. Mutation of the serine to other amino acid residues produces mutants that, while less active than the native enzyme, still exhibit phosphatase activity. When the Zn metals are substituted for softer metals such as Cd²⁺, there is a significant decrease in activity. This observation suggests that the metal atoms within the active site play the most influential role in catalysis.

The catalytic mechanism of AP toward phosphorylated substrates is illustrated in Figure 24. Upon binding of substrate, the phosphate of the substrate forms a phosphate bridge between Zn1 and Zn2 with two of the phosphate oxygens as well as salt bridges with Arg-166. This aligns the phosphate in position so that the conserved serine residue (Ser-102), ideally located opposite the bound substrate, can react with the phosphate in a S_N2 mechanism similar to that observed with the conserved cysteine residue in PTPs to form, in the case of AP, a phosphoserinyl intermediate. Upon expulsion of the leaving group, an activated water molecule that is a ligand to Zn1 hydrolyzes the transient serine-phosphate intermediate to form a second nonenzyme-bound phosphate

intermediate. The last and rate-limiting step in the reaction involves dissociation of phosphate from the metal center to regenerate the active enzyme. As observed in the presence of other nucleophiles, AP also acts as a phosphotransferase to generate other phosphoesters. It is interesting that the catalytic mechanism for APs is a hybridization between the catalytic mechanism employed by PTPs and PPs.

V. Acknowledgments

The authors express their appreciation to Joy Huffman for the initial lessons on the use of the computer programs Swiss Pdb Viewer and POV-Ray. Special thanks are also extended to Dr. Frank Rusnak for reprints of manuscripts that were generously provided on PP2B (calcineurin) structure, mechanism, and regulation. Dr. Kirk Tanner is thanked for his input and critical review of this manuscript. This work was supported in part by the National Institutes of Health (Grant No. GM 59785-01) and the American Heart Association (Grant No. 99603442) to J.M.D.

VI. References

- Hunter, T. *Cell* **1995**, *80*, 225.
- Denu, J. M.; Stuckey, J. A.; Saper, M. A.; Dixon, J. E. *Cell* **1996**, *87*, 361.
- Fauman, E. B.; Yuvaniyama, C.; Schubert, H. L.; Stuckey, J. A.; Saper, M. A. *J. Biol. Chem.* **1996**, *271*, 18780.
- Barford, D. *Trends Biochem. Sci.* **1996**, *21*, 407.
- International Humane Genome Sequencing Consortium. *Nature* **2001**, *409*, 861.
- Rusnak, F.; Mertz, P. *Physiol. Rev.* **2000**, *80*, 1483.
- Denu, J. M.; Dixon, J. E. *Curr. Opin. Chem. Biol.* **1998**, *2*, 633.
- Barford, D.; Neel, B. G. *Structure* **1998**, *6*, 249.
- Ramponi, G.; Stefani, M. *Int. J. Biochem. Cell. Biol.* **1997**, *29*, 279.
- Neel, B. G.; Tonks, N. K. *Curr. Opin. Cell. Biol.* **1997**, *9*, 193.
- Tonks, N. K.; Neel, B. G. *Cell* **1996**, *87*, 365.
- Lohse, D. L.; Denu, J. M.; Dixon, J. E. *Structure* **1995**, *3*, 987.
- Barford, D.; Das, A. K.; Egloff, M. P. *Annu. Rev. Biophys. Biomol. Struct.* **1998**, *27*, 133.
- Bliska, J. B.; Guan, K. L.; Dixon, J. E.; Falkow, S. *Proc. Natl. Acad. Sci. U.S.A.* **1991**, *88*, 1187.
- Zhang, Z. Y.; Clemens, J. C.; Schubert, H. L.; Stuckey, J. A.; Fischer, M. W.; Hume, D. M.; Saper, M. A.; Dixon, J. E. *J. Biol. Chem.* **1992**, *267*, 23759.
- Guan, K. L.; Dixon, J. E. *Science* **1990**, *249*, 553.
- Wiland, A. M.; Denu, J. M.; Mourey, R. J.; Dixon, J. E. *J. Biol. Chem.* **1996**, *271*, 33486.
- Yuvaniyama, J.; Denu, J. M.; Dixon, J. E.; Saper, M. A. *Science* **1996**, *272*, 1328.
- Hof, P.; Pluskey, S.; Dhe-Paganon, S.; Eck, M. J.; Shoelson, S. E. *Cell* **1998**, *92*, 441.
- Bilwes, A. M.; den Hertog, J.; Hunter, T.; Noel, J. P. *Nature* **1996**, *382*, 555.
- Stuckey, J. A.; Schubert, H. L.; Fauman, E. B.; Zhang, Z. Y.; Dixon, J. E.; Saper, M. A. *Nature* **1994**, *370*, 571.
- Barford, D.; Flint, A. J.; Tonks, N. K. *Science* **1994**, *263*, 1397.
- Guex, N.; Peitsch, M. C. *Electrophoresis* **1997**, *18*, 2714.
- Zhou, G.; Denu, J. M.; Wu, L.; Dixon, J. E. *J. Biol. Chem.* **1994**, *269*, 28084.
- Zhang, Z. Y.; Wang, Y.; Wu, L.; Fauman, E. B.; Stuckey, J. A.; Schubert, H. L.; Saper, M. A.; Dixon, J. E. *Biochemistry* **1994**, *33*, 15266.
- Cirri, P.; Chiarugi, P.; Camici, G.; Manao, G.; Raugel, G.; Cappugi, G.; Ramponi, G. *Eur. J. Biochem.* **1993**, *214*, 647.
- Ishibashi, T.; Bottaro, D. P.; Chan, A.; Miki, T.; Aaronson, S. A. *Proc. Natl. Acad. Sci. U.S.A.* **1992**, *89*, 12170.
- Denu, J. M.; Zhou, G.; Guo, Y.; Dixon, J. E. *Biochemistry* **1995**, *34*, 3396.
- Zhang, Z. Y.; Wang, Y.; Dixon, J. E. *Proc. Natl. Acad. Sci. U.S.A.* **1994**, *91*, 1624.
- Taddei, N.; Chiarugi, P.; Cirri, P.; Fiaschi, T.; Stefani, M.; Camici, G.; Raugel, G.; Ramponi, G. *FEBS Lett.* **1994**, *350*, 328.
- Lee, J. O.; Yang, H.; Georgescu, M. M.; Di Cristofano, A.; Maehama, T.; Shi, Y.; Dixon, J. E.; Pandolfi, P.; Pavletich, N. P. *Cell* **1999**, *99*, 323.

- (32) Myers, M. P.; Stolarov, J. P.; Eng, C.; Li, J.; Wang, S. I.; Wigler, M. H.; Parsons, R.; Tonks, N. K. *Proc. Natl. Acad. Sci. U.S.A.* **1997**, *94*, 9052.
- (33) Maehama, T.; Dixon, J. E. *J. Biol. Chem.* **1998**, *273*, 13375.
- (34) Stephens, L. R.; Jackson, T. R.; Hawkins, P. T. *Biochim. Biophys. Acta* **1993**, *1179*, 27.
- (35) Cantley, L. C.; Neel, B. G. *Proc. Natl. Acad. Sci. U.S.A.* **1999**, *96*, 4240.
- (36) Cheney, I. W.; Johnson, D. E.; Vaillancourt, M. T.; Avanzini, J.; Morimoto, A.; Demers, G. W.; Wills, K. N.; Shabram, P. W.; Bolen, J. B.; Tavtigian, S. V.; Bookstein, R. *Cancer Res.* **1998**, *58*, 2331.
- (37) Furnari, F. B.; Lin, H.; Huang, H. S.; Cavenee, W. K. *Proc. Natl. Acad. Sci. U.S.A.* **1997**, *94*, 12479.
- (38) Lee, J. O.; Yang, H.; Georgescu, M. M.; Di Cristofano, A.; Maehama, T.; Shi, Y.; Dixon, J. E.; Pandolfi, P.; Pavletich, N. P. *Cell* **1999**, *99*, 323.
- (39) Cantley, L. C.; Neel, B. G. *Proc. Natl. Acad. Sci. U.S.A.* **1999**, *96*, 4240.
- (40) Zhang, M.; Stauffacher, C. V.; Lin, D.; Van Etten, R. L. *J. Biol. Chem.* **1998**, *273*, 21714.
- (41) Zhang, M.; Zhou, M.; Van Etten, R. L.; Stauffacher, C. V. *Biochemistry* **1997**, *36*, 15.
- (42) Su, X. D.; Taddei, N.; Stefani, M.; Ramponi, G.; Nordlund, P. *Nature* **1994**, *370*, 575.
- (43) Zhang, M.; Van Etten, R. L.; Stauffacher, C. V. *Biochemistry* **1994**, *33*, 11097.
- (44) Wang, S.; Taberner, L.; Zhang, M.; Harms, E.; Van Etten, R. L.; Stauffacher, C. V. *Biochemistry* **2000**, *39*, 1903.
- (45) Stefani, M.; Caselli, A.; Bucciantini, M.; Pazzagli, L.; Dolfi, F.; Camici, G.; Manao, G.; Ramponi, G. *FEBS Lett.* **1993**, *326*, 131.
- (46) Ramponi, G.; Manao, G.; Camici, G.; Cappugi, G.; Ruggiero, M.; Bottaro, D. P. *FEBS Lett.* **1989**, *250*, 469.
- (47) Chernoff, J.; Li, H. C. *Arch. Biochem. Biophys.* **1985**, *240*, 135.
- (48) Ruggiero, M.; Pazzagli, C.; Rigacci, S.; Magnelli, L.; Raugi, G.; Berti, A.; Chiarugi, V. P.; Pierce, J. H.; Camici, G.; Ramponi, G. *FEBS Lett.* **1993**, *326*, 294.
- (49) Ramponi, G.; Ruggiero, M.; Raugi, G.; Berti, A.; Modesti, A.; Degl'Innocenti, D.; Magnelli, L.; Pazzagli, C.; Chiarugi, V. P.; Camici, G. *Int. J. Cancer* **1992**, *51*, 652.
- (50) Fauman, E. B.; Cogswell, J. P.; Lovejoy, B.; Rocque, W. J.; Holmes, W.; Montana, V. G.; Piwnica-Worms, H.; Rink, M. J.; Saper, M. A. *Cell* **1998**, *93*, 617.
- (51) Galaktionov, K.; Beach, D. *Cell* **1991**, *67*, 1181.
- (52) Hoffmann, I.; Clarke, P. R.; Marcote, M. J.; Karsenti, E.; Draetta, G. *EMBO J.* **1993**, *12*, 53.
- (53) Jinno, S.; Suto, K.; Nagata, A.; Igarashi, M.; Kanaoka, Y.; Nojima, H.; Okayama, H. *EMBO J.* **1994**, *13*, 1549.
- (54) Hoffmann, I.; Draetta, G.; Karsenti, E. *EMBO J.* **1994**, *13*, 4302.
- (55) Dunphy, W. G.; Kumagai, A. *Cell* **1991**, *67*, 189.
- (56) Gautier, J.; Solomon, M. J.; Booher, R. N.; Bazan, J. F.; Kirschner, M. W. *Cell* **1991**, *67*, 197.
- (57) Millar, J. B.; McGowan, C. H.; Lenaers, G.; Jones, R.; Russell, P. *EMBO J.* **1991**, *10*, 4301.
- (58) Strausfeld, U.; Labbe, J. C.; Fesquet, D.; Cavadore, J. C.; Picard, A.; Sadhu, K.; Russell, P.; Doree, M. *Nature* **1991**, *351*, 242.
- (59) Bordo, D.; Deriu, D.; Colnaghi, R.; Carpen, A.; Pagani, S.; Bolognesi, M. *J. Mol. Biol.* **2000**, *298*, 691.
- (60) Westley, J. *Adv. Enzymol. Relat. Areas Mol. Biol.* **1973**, *39*, 327.
- (61) Luo, G. X.; Horowitz, P. M. *J. Biol. Chem.* **1994**, *269*, 8220.
- (62) Gottlin, E. B.; Xu, X.; Epstein, D. M.; Burke, S. P.; Eckstein, J. W.; Ballou, D. P.; Dixon, J. E. *J. Biol. Chem.* **1996**, *271*, 27445.
- (63) Hofmann, K.; Bucher, P.; Kajava, A. V. *J. Mol. Biol.* **1998**, *282*, 195.
- (64) Reynolds, R. A.; Yem, A. W.; Wolfe, C. L.; Deibel, M. R., Jr.; Chidester, C. G.; Watenpugh, K. D. *J. Mol. Biol.* **1999**, *293*, 559.
- (65) Chen, W.; Wilborn, M.; Rudolph, J. *Biochemistry* **2000**, *39*, 10781.
- (66) Brady-Kalnay, S. M.; Rimm, D. L.; Tonks, N. K. *J. Cell Biol.* **1995**, *130*, 977.
- (67) Sap, J.; Jiang, Y. P.; Friedlander, D.; Grumet, M.; Schlessinger, J. *Mol. Cell. Biol.* **1994**, *14*, 1.
- (68) Cheng, J.; Wu, K.; Armanini, M.; O'Rourke, N.; Dowbenko, D.; Lasky, L. A. *J. Biol. Chem.* **1997**, *272*, 7264.
- (69) Fuchs, M.; Muller, T.; Lerch, M. M.; Ullrich, A. *J. Biol. Chem.* **1996**, *271*, 16712.
- (70) Kokel, M.; Borland, C. Z.; DeLong, L.; Horvitz, H. R.; Stern, M. *J. Genes Dev.* **1998**, *12*, 1425.
- (71) Desai, D. M.; Sap, J.; Silvennoinen, O.; Schlessinger, J.; Weiss, A. *EMBO J.* **1994**, *13*, 4002.
- (72) den Hertog, J.; Pals, C. E.; Peppelenbosch, M. P.; Tertoolen, L. G.; de Laat, S. W.; Kruijer, W. *EMBO J.* **1993**, *12*, 3789.
- (73) Levy, J. B.; Canoll, P. D.; Silvennoinen, O.; Barnea, G.; Morse, B.; Honegger, A. M.; Huang, J. T.; Cannizzaro, L. A.; Park, S. H.; Druck, T. and others. *J. Biol. Chem.* **1993**, *268*, 10573.
- (74) Krueger, N. X.; Streuli, M.; Saito, H. *EMBO J.* **1990**, *9*, 3241.
- (75) Buist, A.; Zhang, Y. L.; Keng, Y. F.; Wu, L.; Zhang, Z. Y.; den Hertog, J. *Biochemistry* **1999**, *38*, 914.
- (76) Kwak, S. P.; Hakes, D. J.; Martell, K. J.; Dixon, J. E. *J. Biol. Chem.* **1994**, *269*, 3596.
- (77) Keyse, S. M.; Ginsburg, M. *Trends Biochem. Sci.* **1993**, *18*, 377.
- (78) Groom, L. A.; Sneddon, A. A.; Alessi, D. R.; Dowd, S.; Keyse, S. M. *EMBO J.* **1996**, *15*, 3621.
- (79) Muda, M.; Theodosiou, A.; Rodrigues, N.; Boschert, U.; Camps, M.; Gillieron, C.; Davies, K.; Ashworth, A.; Arkinstall, S. *J. Biol. Chem.* **1996**, *271*, 27205.
- (80) Muda, M.; Theodosiou, A.; Gillieron, C.; Smith, A.; Chabert, C.; Camps, M.; Boschert, U.; Rodrigues, N.; Davies, K.; Ashworth, A.; Arkinstall, S. *J. Biol. Chem.* **1998**, *273*, 9323.
- (81) Jia, Z.; Barford, D.; Flint, A. J.; Tonks, N. K. *Science* **1995**, *268*, 1754.
- (82) Chen, L.; Montserat, J.; Lawrence, D. S.; Zhang, Z. Y. *Biochemistry* **1996**, *35*, 9349.
- (83) Tenev, T.; Keilhack, H.; Tomic, S.; Stoyanov, B.; Stein-Gerlach, M.; Lammers, R.; Krivtsov, A. V.; Ullrich, A.; Bohmer, F. D. *J. Biol. Chem.* **1997**, *272*, 5966.
- (84) O'Reilly, A. M.; Neel, B. G. *Mol. Cell. Biol.* **1998**, *18*, 161.
- (85) Garton, A. J.; Flint, A. J.; Tonks, N. K. *Mol. Cell. Biol.* **1996**, *16*, 6408.
- (86) Tiganis, T.; Bennett, A. M.; Ravichandran, K. S.; Tonks, N. K. *Mol. Cell. Biol.* **1998**, *18*, 1622.
- (87) Zhang, Z. Y.; Maclean, D.; Thieme-Sefler, A. M.; Roeske, R. W.; Dixon, J. E. *Anal. Biochem.* **1993**, *211*, 7.
- (88) Zhang, Z. Y.; Thieme-Sefler, A. M.; Maclean, D.; McNamara, D. J.; Dobrusin, E. M.; Sawyer, T. K.; Dixon, J. E. *Proc. Natl. Acad. Sci. U.S.A.* **1993**, *90*, 4446.
- (89) Vetter, S. W.; Keng, Y. F.; Lawrence, D. S.; Zhang, Z. Y. *J. Biol. Chem.* **2000**, *275*, 2265.
- (90) Sarmiento, M.; Zhao, Y.; Gordon, S. J.; Zhang, Z. Y. *J. Biol. Chem.* **1998**, *273*, 26368.
- (91) Sarmiento, M.; Puius, Y. A.; Vetter, S. W.; Keng, Y. F.; Wu, L.; Zhao, Y.; Lawrence, D. S.; Almo, S. C.; Zhang, Z. Y. *Biochemistry* **2000**, *39*, 8171.
- (92) Peters, G. H.; Iversen, L. F.; Branner, S.; Andersen, H. S.; Mortensen, S. B.; Olsen, O. H.; Moller, K. B.; Moller, N. P. *J. Biol. Chem.* **2000**, *275*, 18201.
- (93) Denu, J. M.; Zhou, G.; Wu, L.; Zhao, R.; Yuvaniyama, J.; Saper, M. A.; Dixon, J. E. *J. Biol. Chem.* **1995**, *270*, 3796.
- (94) Riordan, J. F.; McElvany, K. D.; Borders, C. L., Jr. *Science* **1977**, *195*, 884.
- (95) Byon, J. C.; Kusari, A. B.; Kusari, J. *Mol. Cell. Biochem.* **1998**, *182*, 101.
- (96) Salmeen, A.; Andersen, J. N.; Myers, M. P.; Tonks, N. K.; Barford, D. *Mol. Cell* **2000**, *6*, 1401.
- (97) Streuli, M.; Krueger, N. X.; Tsai, A. Y.; Saito, H. *Proc. Natl. Acad. Sci. U.S.A.* **1989**, *86*, 8698.
- (98) Streuli, M.; Krueger, N. X.; Thai, T.; Tang, M.; Saito, H. *EMBO J.* **1990**, *9*, 2399.
- (99) Gebbink, M. F.; Verheijen, M. H.; Zondag, G. C.; van Etten, I.; Moolenaar, W. H. *Biochemistry* **1993**, *32*, 13516.
- (100) Guan, K. L.; Dixon, J. E. *J. Biol. Chem.* **1991**, *266*, 17026.
- (101) Zhang, Z. Y.; Dixon, J. E. *Biochemistry* **1993**, *32*, 9340.
- (102) Zhang, Z. Y.; Palfey, B. A.; Wu, L.; Zhao, Y. *Biochemistry* **1995**, *34*, 16389.
- (103) Peters, G. H.; Frimurer, T. M.; Olsen, O. H. *Biochemistry* **1998**, *37*, 5383.
- (104) Denu, J. M.; Lohse, D. L.; Vijayalakshmi, J.; Saper, M. A.; Dixon, J. E. *Proc. Natl. Acad. Sci. U.S.A.* **1996**, *93*, 2493.
- (105) Cho, H.; Krishnaraj, R.; Kitas, E.; Bannwarth, W.; Walsh, C. T.; Anderson, K. S. *J. Am. Chem. Soc.* **1992**, *114*, 7296.
- (106) Pannifer, A. D.; Flint, A. J.; Tonks, N. K.; Barford, D. *J. Biol. Chem.* **1998**, *273*, 10454.
- (107) Lohse, D. L.; Denu, J. M.; Santoro, N.; Dixon, J. E. *Biochemistry* **1997**, *36*, 4568.
- (108) Eckstein, J. W.; Beer-Romero, P.; Berdo, I. *Protein Sci.* **1996**, *5*, 5.
- (109) Cleland, W. W. *FASEB J.* **1990**, *4*, 2899.
- (110) Gorenstein, D. G.; Lee, Y.-G.; Kar, D. *J. Am. Chem. Soc.* **1977**, *99*, 2264.
- (111) Kirby, A. J.; Varvoglis, A. G. *J. Am. Chem. Soc.* **1967**, *89*, 415.
- (112) Bunton, C. A.; Fendler, E. J.; Humeres, E.; Yang, K.-U. *J. Org. Chem.* **1967**, *32*, 2806.
- (113) Butcher, W. W.; Westheimer, F. H. *J. Am. Chem. Soc.* **1955**, *77*, 2420.
- (114) Hengge, A. C.; Edens, W. A.; Elsing, H. *J. Am. Chem. Soc.* **1994**, *116*, 5045.
- (115) Hassett, A.; Blattler, W.; Knowles, J. R. *Biochemistry* **1982**, *21*, 6335.
- (116) Knowles, J. R. *Annu. Rev. Biochem.* **1980**, *49*, 877.
- (117) Han, R.; Coleman, J. E. *Biochemistry* **1995**, *34*, 4238.
- (118) Hengge, A. C.; Sowa, G. A.; Wu, L.; Zhang, Z. Y. *Biochemistry* **1995**, *34*, 13982.
- (119) Hengge, A. C.; Denu, J. M.; Dixon, J. E. *Biochemistry* **1996**, *35*, 7084.
- (120) Hengge, A. C.; Zhao, Y.; Wu, L.; Zhang, Z. Y. *Biochemistry* **1997**, *36*, 7928.

- (121) Mondesert, O.; Moreno, S.; Russell, P. *J. Biol. Chem.* **1994**, *269*, 27996.
- (122) Wu, L.; Zhang, Z. Y. *Biochemistry* **1996**, *35*, 5426.
- (123) Denu, J. M.; Dixon, J. E. *Proc. Natl. Acad. Sci. U.S.A.* **1995**, *92*, 5910.
- (124) Keng, Y. F.; Wu, L.; Zhang, Z. Y. *Eur. J. Biochem.* **1999**, *259*, 809.
- (125) Hoff, R. H.; Hengge, A. C.; Wu, L.; Keng, Y. F.; Zhang, Z. Y. *Biochemistry* **2000**, *39*, 46.
- (126) Stewart, A. E.; Dowd, S.; Keyse, S. M.; McDonald, N. Q. *Nat. Struct. Biol.* **1999**, *6*, 174.
- (127) Fjeld, C. C.; Rice, A. E.; Kim, Y.; Gee, K. R.; Denu, J. M. *J. Biol. Chem.* **2000**, *275*, 6749.
- (128) Zhao, Y.; Zhang, Z. Y. *Biochemistry* **1996**, *35*, 11797.
- (129) Wu, L.; Zhang, Z. Y. *Biochemistry* **1996**, *35*, 5426.
- (130) Zhang, Z. Y.; VanEtten, R. L. *J. Biol. Chem.* **1991**, *266*, 1516.
- (131) Jencks, W. P.; Gilchert, M. J. *Am. Chem. Soc.* **1968**, *90*, 2622.
- (132) Herschlag, D.; Jencks, W. P. *J. Am. Chem. Soc.* **1989**, *111*, 7579.
- (133) Kirby, A. J.; Jencks, W. P. *J. Am. Chem. Soc.* **1965**, *87*, 3209.
- (134) Cleland, W. W.; Hengge, A. C. *FASEB J.* **1995**, *9*, 1585.
- (135) Khan, S. A.; Kirby, A. J. *J. Chem. Soc. B* **1970**, 1172.
- (136) Camps, M.; Nichols, A.; Gillieron, C.; Antonsson, B.; Muda, M.; Chabert, C.; Boschert, U.; Arkininstall, S. *Science* **1998**, *280*, 1262.
- (137) Zhou, B.; Zhang, Z. Y. *J. Biol. Chem.* **1999**, *274*, 35526.
- (138) Rigas, J. D.; Hoff, R. H.; Rice, A. E.; Hengge, A. C.; Denu, J. M. *Biochemistry* **2001**, *39*, 10781.
- (139) Nichols, A.; Camps, M.; Gillieron, C.; Chabert, C.; Brunet, A.; Wilsbacher, J.; Cobb, M.; Pouyssegur, J.; Shaw, J. P.; Arkininstall, S. *J. Biol. Chem.* **2000**, *275*, 24613.
- (140) Zhou, B.; Wu, L.; Shen, K.; Zhang, J.; Lawrence, D. S.; Zhang, Z. Y. *J. Biol. Chem.* **2001**, *276*, 6506.
- (141) Farooq, A.; Chaturvedi, G.; Mujtaha, S.; Plotnikova, O.; Zeng, L.; Dhalluin, C.; Ashton, R.; Zhou, M. *Mol. Cell* **2001**, *7*, 387.
- (142) Hoffmann, K. M.; Tonks, N. K.; Barford, D. *J. Biol. Chem.* **1997**, *272*, 27505.
- (143) Majeti, R.; Bilwes, A. M.; Noel, J. P.; Hunter, T.; Weiss, A. *Science* **1998**, *279*, 88.
- (144) Desai, D. M.; Sap, J.; Schlessinger, J.; Weiss, A. *Cell* **1993**, *73*, 541.
- (145) Takeda, A.; Wu, J. J.; Maizel, A. L. *J. Biol. Chem.* **1992**, *267*, 16651.
- (146) Felberg, J.; Johnson, P. *J. Biol. Chem.* **1998**, *273*, 17839.
- (147) Jiang, G.; den Hertog, J.; Su, J.; Noel, J.; Sap, J.; Hunter, T. *Nature* **1999**, *401*, 606.
- (148) Jiang, G.; den Hertog, J.; Hunter, T. *Mol. Cell. Biol.* **2000**, *20*, 5917.
- (149) Wallace, M. J.; Fladd, C.; Batt, J.; Rotin, D. *Mol. Cell. Biol.* **1998**, *18*, 2608.
- (150) Blanchetot, C.; den Hertog, J. *J. Biol. Chem.* **2000**, *275*, 12446.
- (151) Meng, K.; Rodriguez-Pena, A.; Dimitrov, T.; Chen, W.; Yamin, M.; Noda, M.; Deuel, T. F. *Proc. Natl. Acad. Sci. U.S.A.* **2000**, *97*, 2603.
- (152) Meng, K.; Rodriguez-Pena, A.; Dimitrov, T.; Chen, W.; Yamin, M.; Noda, M.; Deuel, T. F. *Proc. Natl. Acad. Sci. U.S.A.* **2000**, *97*, 2603.
- (153) Feiken, E.; van Etten, I.; Gebbink, M. F.; Moolenaar, W. H.; Zondag, G. C. *J. Biol. Chem.* **2000**, *275*, 15350.
- (154) Wang, Y.; Pallen, C. J. *EMBO J.* **1991**, *10*, 3231.
- (155) Sugimoto, S.; Lechleider, R. J.; Shoelson, S. E.; Neel, B. G.; Walsh, C. T. *J. Biol. Chem.* **1993**, *268*, 22771.
- (156) Pluskey, S.; Wandless, T. J.; Walsh, C. T.; Shoelson, S. E. *J. Biol. Chem.* **1995**, *270*, 2897.
- (157) Lechleider, R. J.; Sugimoto, S.; Bennett, A. M.; Kashishian, A. S.; Cooper, J. A.; Shoelson, S. E.; Walsh, C. T.; Neel, B. G. *J. Biol. Chem.* **1993**, *268*, 21478.
- (158) Eck, M. J.; Pluskey, S.; Trub, T.; Harrison, S. C.; Shoelson, S. E. *Nature* **1996**, *379*, 277.
- (159) Lee, C. H.; Kominos, D.; Jacques, S.; Margolis, B.; Schlessinger, J.; Shoelson, S. E.; Kuriyan, J. *Structure* **1994**, *2*, 423.
- (160) Suzuki, Y. J.; Forman, H. J.; Sevanian, A. *Free Radical Biol. Med.* **1997**, *22*, 269.
- (161) Irani, K.; Xia, Y.; Zweier, J. L.; Sollott, S. J.; Der, C. J.; Fearon, E. R.; Sundaresan, M.; Finkel, T.; Goldschmidt-Clermont, P. J. *Science* **1997**, *275*, 1649.
- (162) Heffetz, D.; Bushkin, I.; Dror, R.; Zick, Y. *J. Biol. Chem.* **1990**, *265*, 2896.
- (163) Knebel, A.; Rahmsdorf, H. J.; Ullrich, A.; Herrlich, P. *EMBO J.* **1996**, *15*, 5314.
- (164) Denu, J. M.; Tanner, K. G. *Biochemistry* **1998**, *37*, 5633.
- (165) Bae, Y. S.; Kang, S. W.; Seo, M. S.; Baines, I. C.; Tekle, E.; Chock, P. B.; Rhee, S. G. *J. Biol. Chem.* **1997**, *272*, 217.
- (166) Sundaresan, M.; Yu, Z. X.; Ferrans, V. J.; Sulciner, D. J.; Gutkind, J. S.; Irani, K.; Goldschmidt-Clermont, P. J.; Finkel, T. *Biochem. J.* **1996**, *318*, 379.
- (167) Lo, Y. Y.; Cruz, T. F. *J. Biol. Chem.* **1995**, *270*, 11277.
- (168) Sullivan, S. G.; Chiu, D. T.; Errasfa, M.; Wang, J. M.; Qi, J. S.; Stern, A. *Free Radical Biol. Med.* **1994**, *16*, 399.
- (169) Hecht, D.; Zick, Y. *Biochem. Biophys. Res. Commun.* **1992**, *188*, 773.
- (170) Lee, S. R.; Kwon, K. S.; Kim, S. R.; Rhee, S. G. *J. Biol. Chem.* **1998**, *273*, 15366.
- (171) Ellis, H. R.; Poole, L. B. *Biochemistry* **1997**, *36*, 15013.
- (172) Barrett, W. C.; DeGnore, J. P.; Konig, S.; Fales, H. M.; Keng, Y. F.; Zhang, Z. Y.; Yim, M. B.; Chock, P. B. *Biochemistry* **1999**, *38*, 6699.
- (173) Ostergaard, H. L.; Trowbridge, I. S. *Science* **1991**, *253*, 1423.
- (174) Stover, D. R.; Charbonneau, H.; Tonks, N. K.; Walsh, K. A. *Proc. Natl. Acad. Sci. U.S.A.* **1991**, *88*, 7704.
- (175) Autero, M.; Gahmberg, C. G. *Eur. J. Immunol.* **1987**, *17*, 1503.
- (176) Ouyang, B.; Li, W.; Pan, H.; Meadows, J.; Hoffmann, I.; Dai, W. *Oncogene* **1999**, *18*, 6029.
- (177) Ouyang, B.; Pan, H.; Lu, L.; Li, J.; Stambrook, P.; Li, B.; Dai, W. *J. Biol. Chem.* **1997**, *272*, 28646.
- (178) Baldin, V.; Cans, C.; Knibiehler, M.; Ducommun, B. *J. Biol. Chem.* **1997**, *272*, 32731.
- (179) Gabrielli, B. G.; Clark, J. M.; McCormack, A. K.; Ellem, K. A. *J. Biol. Chem.* **1997**, *272*, 28607.
- (180) Nishijima, H.; Nishitani, H.; Seki, T.; Nishimoto, T. *J. Cell Biol.* **1997**, *138*, 1105.
- (181) Brondello, J. M.; Pouyssegur, J.; McKenzie, F. R. *Science* **1999**, *286*, 2514.
- (182) Flint, A. J.; Gebbink, M. F.; Franza, B. R., Jr.; Hill, D. E.; Tonks, N. K. *EMBO J.* **1993**, *12*, 1937.
- (183) Shifrin, V. I.; Davis, R. J.; Neel, B. G. *J. Biol. Chem.* **1997**, *272*, 2957.
- (184) Moeslein, F. M.; Myers, M. P.; Landreth, G. E. *J. Biol. Chem.* **1999**, *274*, 26697.
- (185) Kenner, K. A.; Anyanwu, E.; Olefsky, J. M.; Kusari, J. *J. Biol. Chem.* **1996**, *271*, 19810.
- (186) Liu, F.; Chernoff, J. *Biochem. J.* **1997**, *327*, 139.
- (187) Bennett, A. M.; Tang, T. L.; Sugimoto, S.; Walsh, C. T.; Neel, B. G. *Proc. Natl. Acad. Sci. U.S.A.* **1994**, *91*, 7335.
- (188) den Hertog, J.; Tracy, S.; Hunter, T. *EMBO J.* **1994**, *13*, 3020.
- (189) Rusnak, F. *Met. Ions. Biol. Syst.* **2000**, *37*, 305.
- (190) Cohen, P.; Cohen, P. T. *J. Biol. Chem.* **1989**, *264*, 21435.
- (191) Cohen, P. *Annu. Rev. Biochem.* **1989**, *58*, 453.
- (192) Cohen, P. T. *Trends Biochem. Sci.* **1997**, *22*, 245.
- (193) Shenolikar, S. *Annu. Rev. Cell Biol.* **1994**, *10*, 55.
- (194) Bollen, M.; Stalmans, W. *Crit. Rev. Biochem. Mol. Biol.* **1992**, *27*, 227.
- (195) Haystead, T. A.; Sim, A. T.; Carling, D.; Honnor, R. C.; Tsukitani, Y.; Cohen, P.; Hardie, D. G. *Nature* **1989**, *337*, 78.
- (196) Mayer-Jaekel, R. E.; Ohkura, H.; Gomes, R.; Sunkel, C. E.; Baumgartner, S.; Hemmings, B. A.; Glover, D. M. *Cell* **1993**, *72*, 621.
- (197) Sontag, E.; Fedorov, S.; Kamibayashi, C.; Robbins, D.; Cobb, M.; Mumby, M. *Cell* **1993**, *75*, 887.
- (198) Crabtree, G. R.; Clipstone, N. A. *Annu. Rev. Biochem.* **1994**, *63*, 1045.
- (199) Schreiber, S. L.; Crabtree, G. R. *Immunol. Today* **1992**, *13*, 136.
- (200) Chernoff, J.; Sells, M. A.; Li, H. C. *Biochem. Biophys. Res. Commun.* **1984**, *121*, 141.
- (201) Li, H. C. *J. Biol. Chem.* **1984**, *259*, 8801.
- (202) Stewart, A. A.; Ingebritsen, T. S.; Cohen, P. *Eur. J. Biochem.* **1983**, *132*, 289.
- (203) Stewart, A. A.; Ingebritsen, T. S.; Manalan, A.; Klee, C. B.; Cohen, P. *FEBS Lett.* **1982**, *137*, 80.
- (204) Friedman, J.; Weissman, I. *Cell* **1991**, *66*, 799.
- (205) Liu, J.; Farmer, J. D., Jr.; Lane, W. S.; Friedman, J.; Weissman, I.; Schreiber, S. L. *Cell* **1991**, *66*, 807.
- (206) Bork, P.; Brown, N. P.; Hegyi, H.; Schultz, J. *Protein Sci.* **1996**, *5*, 1421.
- (207) Cohen, P.; Klumpp, S.; Schelling, D. L. *FEBS Lett.* **1989**, *250*, 596.
- (208) Peruski, L. F. *Adv. Protein Phosphatases* **1993**, *7*, 9.
- (209) Kato, S.; Terasawa, T.; Kobayashi, T.; Ohnishi, M.; Sasahara, Y.; Kusuda, K.; Yanagawa, Y.; Hiraga, A.; Matsui, Y.; Tamura, S. *Arch. Biochem. Biophys.* **1995**, *318*, 387.
- (210) Hou, E. W.; Kawai, Y.; Miyasaka, H.; Li, S. S. *Biochem. Mol. Biol. Int.* **1994**, *32*, 773.
- (211) Terasawa, T.; Kobayashi, T.; Murakami, T.; Ohnishi, M.; Kato, S.; Tanaka, O.; Kondo, H.; Yamamoto, H.; Takeuchi, T.; Tamura, S. *Arch. Biochem. Biophys.* **1993**, *307*, 342.
- (212) Meskiene, I.; Bogre, L.; Glaser, W.; Balog, J.; Brandstotter, M.; Zwerger, K.; Ammerer, G.; Hirt, H. *Proc. Natl. Acad. Sci. U.S.A.* **1998**, *95*, 1938.
- (213) Shiozaki, K.; Russell, P. *EMBO J.* **1995**, *14*, 492.
- (214) Gaits, F.; Shiozaki, K.; Russell, P. *J. Biol. Chem.* **1997**, *272*, 17873.
- (215) Takekawa, M.; Maeda, T.; Saito, H. *EMBO J.* **1998**, *17*, 4744.
- (216) Hanada, M.; Kobayashi, T.; Ohnishi, M.; Ikeda, S.; Wang, H.; Katsura, K.; Yanagawa, Y.; Hiraga, A.; Kanamaru, R.; Tamura, S. *FEBS Lett.* **1998**, *437*, 172.
- (217) Zhuo, S.; Clemens, J. C.; Stone, R. L.; Dixon, J. E. *J. Biol. Chem.* **1994**, *269*, 26234.
- (218) Koonin, E. V. *Protein Sci.* **1994**, *3*, 356.
- (219) Goldberg, J.; Huang, H. B.; Kwon, Y. G.; Greengard, P.; Nairn, A. C.; Kuriyan, J. *Nature* **1995**, *376*, 745.

- (220) Egloff, M. P.; Cohen, P. T.; Reinemer, P.; Barford, D. *J. Mol. Biol.* **1995**, *254*, 942.
- (221) Griffith, J. P.; Kim, J. L.; Kim, E. E.; Sintchak, M. D.; Thomson, J. A.; Fitzgibbon, M. J.; Fleming, M. A.; Caron, P. R.; Hsiao, K.; Navia, M. A. *Cell* **1995**, *82*, 507.
- (222) Kissinger, C. R.; Parge, H. E.; Knighton, D. R.; Lewis, C. T.; Pelletier, L. A.; Tempczyk, A.; Kalish, V. J.; Tucker, K. D.; Showalter, R. E.; Moomaw, E. W.; et al. *Nature* **1995**, *378*, 641.
- (223) King, M. M.; Huang, C. Y. *J. Biol. Chem.* **1984**, *259*, 8847.
- (224) Uppenberg, J.; Lindqvist, F.; Svensson, C.; Ek-Rylander, B.; Andersson, G. *J. Mol. Biol.* **1999**, *290*, 201.
- (225) Klabunde, T.; Strater, N.; Frohlich, R.; Witzel, H.; Krebs, B. *J. Mol. Biol.* **1996**, *259*, 737.
- (226) Sträter, N.; Klabunde, T.; Tucker, P.; Witzel, H.; Krebs, B. *Science* **1995**, *268*, 1489.
- (227) Klabunde, T.; Krebs, B. *Struct. Bonding* **1997**, *89*, 177.
- (228) Martin, B.; Pallen, C. J.; Wang, J. H.; Graves, D. J. *J. Biol. Chem.* **1985**, *260*, 14932.
- (229) Lynn, K. R.; Clevette-Radford, N. A.; Chuaqui, C. A. *Bioorg. Chem.* **1981**, *10*, 90.
- (230) Hsu, R. Y.; Cleland, W. W.; Anderson, L. *Biochemistry* **1966**, *5*, 799.
- (231) Williams, A.; Naylor, R. A.; Collyer, S. G. *J. Chem. Soc., Perkin Trans. 2* **1973**, 25.
- (232) Martin, B. L.; Graves, D. J. *J. Biol. Chem.* **1986**, *261*, 14545.
- (233) Rudolph, F. B. *Methods Enzymol.* **1979**, *63*, 411.
- (234) Mueller, E. G.; Crowder, M. W.; Averill, B. A.; Knowles, J. R. *J. Am. Chem. Soc.* **1993**, *115*, 2974.
- (235) Martin, B. L.; Graves, D. J. *Biochim. Biophys. Acta* **1994**, *1206*, 136.
- (236) Pinkse, M. W.; Merckx, M.; Averill, B. A. *Biochemistry* **1999**, *38*, 9926.
- (237) Wang, X.; Ho, R. Y. N.; Whiting, A. K.; Que, L., Jr. *J. Am. Chem. Soc.* **1999**, *121*, 9235.
- (238) Wahnou, D.; Lebuis, A.-M.; Chin, J. *Angew. Chem., Int. Ed. Engl.* **1995**, *34*, 2412.
- (239) Williams, N. H.; Chin, J. *J. Chem. Soc., Chem. Commun.* **1996**, 131.
- (240) Williams, N. H.; Cheung, W.; Chin, J. *J. Am. Chem. Soc.* **1998**, *120*, 0, 8079.
- (241) Huang, H. B.; Horiuchi, A.; Goldberg, J.; Greengard, P.; Nairn, A. C. *Proc. Natl. Acad. Sci. U.S.A.* **1997**, *94*, 3530.
- (242) Zhang, J.; Zhang, Z.; Brew, K.; Lee, E. Y. *Biochemistry* **1996**, *35*, 6276.
- (243) Mondragon, A.; Griffith, E. C.; Sun, L.; Xiong, F.; Armstrong, C.; Liu, J. O. *Biochemistry* **1997**, *36*, 4934.
- (244) Mertz, P.; Yu, L.; Sikkink, R.; Rusnak, F. *J. Biol. Chem.* **1997**, *272*, 21296.
- (245) Hengge, A. C.; Martin, B. L. *Biochemistry* **1997**, *36*, 10185.
- (246) Hoff, R. H.; Mertz, P.; Rusnak, F.; Hengge, A. C. *J. Am. Chem. Soc.* **1999**, *121*, 6382.
- (247) Tsuiki, S.; Hiraga, A.; Kikuchi, K.; Tamura, S. *Methods. Enzymol.* **1988**, *159*, 437.
- (248) Hiraga, A.; Kikuchi, K.; Tamura, S.; Tsuiki, S. *Eur. J. Biochem.* **1981**, *119*, 503.
- (249) Tamura, S.; Tsuiki, S. *Eur. J. Biochem.* **1980**, *111*, 217.
- (250) Tamura, S.; Kikuchi, H.; Kikuchi, K.; Hiraga, A.; Tsuiki, S. *Eur. J. Biochem.* **1980**, *104*, 347.
- (251) Mann, D. J.; Campbell, D. G.; McGowan, C. H.; Cohen, P. T. *Biochim. Biophys. Acta* **1992**, *1130*, 100.
- (252) Wenk, J.; Trompeter, H. I.; Pettrich, K. G.; Cohen, P. T.; Campbell, D. G.; Mieskes, G. *FEBS Lett.* **1992**, *297*, 135.
- (253) Tamura, S.; Lynch, K. R.; Lerner, J.; Fox, J.; Yasui, A.; Kikuchi, K.; Suzuki, Y.; Tsuiki, S. *Proc. Natl. Acad. Sci. U.S.A.* **1989**, *86*, 1796.
- (254) Travis, S. M.; Welsh, M. J. *FEBS Lett.* **1997**, *412*, 415.
- (255) Das, A. K.; Helps, N. R.; Cohen, P. T.; Barford, D. *EMBO J.* **1996**, *15*, 6798.
- (256) Fjeld, C. C.; Denu, J. M. *J. Biol. Chem.* **1999**, *274*, 20336.
- (257) Pato, M. D.; Kerc, E. *Mol. Cell. Biochem.* **1991**, *101*, 31.
- (258) Fjeld, C. C.; Denu, J. M. *J. Biol. Chem.* **1999**, *274*, 20336.
- (259) Pohjanjoki, P.; Lahti, R.; Goldman, A.; Cooperman, B. S. *Biochemistry* **1998**, *37*, 1754.
- (260) Chen, G.; Edwards, T.; D'souza, V. M.; Holz, R. C. *Biochemistry* **1997**, *36*, 4278.
- (261) Kobayashi, T.; Kanno, S.; Terasawa, T.; Murakami, T.; Ohnishi, M.; Ohtsuki, K.; Hiraga, A.; Tamura, S. *Biochem. Biophys. Res. Commun.* **1993**, *195*, 484.
- (262) Kobayashi, T.; Kusuda, K.; Ohnishi, M.; Wang, H.; Ikeda, S.; Hanada, M.; Yanagawa, Y.; Tamura, S. *FEBS Lett.* **1998**, *430*, 222.
- (263) Merckx, M.; Averill, B. A. *Biochemistry* **1998**, *37*, 11223.
- (264) Yu, L.; Golbeck, J.; Yao, J.; Rusnak, F. *Biochemistry* **1997**, *36*, 10727.
- (265) Wang, X.; Culotta, V. C.; Klee, C. B. *Nature* **1996**, *383*, 434.
- (266) Sommer, D.; Fakata, K. L.; Swanson, S. A.; Stemmer, P. M. *Eur. J. Biochem.* **2000**, *267*, 2312.
- (267) Ferri, A.; Gabbianelli, R.; Casciati, A.; Paolucci, E.; Rotilio, G.; Carri, M. T. *J. Neurochem.* **2000**, *75*, 606.
- (268) Iwai, K.; Drake, S. K.; Wehr, N. B.; Weissman, A. M.; LaVaute, T.; Minato, N.; Klausner, R. D.; Levine, R. L.; Rouault, T. A. *Proc. Natl. Acad. Sci. U.S.A.* **1998**, *95*, 4924.
- (269) Uchida, K.; Kawakishi, S. *J. Biol. Chem.* **1994**, *269*, 2405.
- (270) Cabisco, E.; Aguilar, J.; Ros, J. *J. Biol. Chem.* **1994**, *269*, 6592.
- (271) Holtz, K. M.; Kantrowitz, E. R. *FEBS Lett.* **1999**, *462*, 7.
- (272) Coleman, J. E. *Annu. Rev. Biophys. Biomol. Struct.* **1992**, *21*, 441.

CR000247E